GEOLOGICAL SURVEY OF CANADA

OPEN FILE 3144

Metallogeny of base metal deposits of the Abitibi Greenstone Belt

Edited by G. Tourigny

1995

Natural Resources Canada Ressources naturelles Canada

Canada

PRECAMBRIAN '95

METALLOGENY OF BASE METAL DEPOSITS OF THE ABITIBI GREENSTONE BELT

Field Trip Guidebook

edited by
Ghislain Tourigny

with contributions from:
Edmund Stuart, Peter Pelz, Yves Rougerie, Louis Martin,
André Bonenfant, Sergio Cattalani, J. Lacroix, and R. Daigneault

Geological Survey of Canada
Open File 3144

TABLE OF CONTENTS

Preface

Archean volcanic complexes characterized by mafic and felsic flows, hyaloclastites and fragmental volcanic rocks of the Abitibi greenstone belt have received much attention and have been the object of rejuvenated base metal exploration activity during the last decade. This renewed interest in volcanogenic massive sulphide (VMS) mineralization is due mainly to the increase in the price of base metals, but also due to the recent recognizition that these deposits may occur in a variety of stratigraphic and structural settings. The purpose of this field trip is to give participants an understanding of these geological and structural settings for VMS deposits in the Abitibi greenstone belt. Deposits in various stratigraphic and structural settings will be visited to illustrate similarities and differences between them.

The field trip is organized into two sections. The first includes underground tours of weakly deformed volcanogenic massive sulphide deposits at the Isle-Dieu (Matagami district). The second is devoted to the complexely deformed Bousquet #2 (Cadillac district), Louvicourt and Grevet mines (Val-d'Or district). Visits of excellent surface exposures on the Bousquet and Val-d'Or mining camps are also expected. A visit to a deformed granulite-grade massive sulphide showing in the Grenville Province is also planned. The outcrops visited will give the participants an opportunity to acquaint themselves with the regional geological settings of the deposits.

Editor

Ghislain Tourigny

Geology of the Bousquet #2, Au-Ag-Cu deposit

by Nick Teasdale[1], Ghislain Tourigny[2], Alex Brown[1], Louis Gauthier[3] and Gérald Panneton[3]

[1] Département de génie minéral, École Polytechnique de Montréal, C.P. 6079, succ. A, Montréal (Québec), Canada, H3C 3A7

[2] Ministère des Ressources Naturelles du Québec, Service Géologique du nord-ouest, 400 blv. Lamaque, Val-d'Or (Québec), Canada, J9P 3L4

[3] American Barrick Resources Corporation, Eastern Canada Exploration, 2 chemin Bousquet, Route 395, Preissac (Québec), Canada, J0Y 2E0

Introduction

The Bousquet #2 mine is a typical pyritic gold-copper deposit located in the Cadillac mining district in the eastern Abitibi belt. Since 1990, the mine has produced over 741,000 ounces of gold and 27,000 tons of Cu from strongly deformed massive and semi-massive pyritic lenses. The ore reserves at the end of 1993 were estimated at 7.7 Mt grading 0.19 g/t Au and 0.45 % Cu (D. Doucet, pers. comm, 1995). This Au-Ag-Cu deposit represents the western downplunge extension of the Dumagami orebody which has been described recently by Marquis et al. (1990a, 1990b).

Along with the adjacent Doyon and Dumagami mines, the Bousquet #2 deposit is located within a zone of intense ductile-brittle deformation (Tourigny, 1991). Although these deposits have received much attention in recent years (see Valliant, 1981; Valliant et al., 1983; Eliopoulos, 1983; Bateman, 1984; Savoie et al., 1986; Stone, 1988; Tourigny et al., 1988, 1989a, 1989b, 1993; Marquis, 1990; Marquis et al., 1990a, 1990b), many uncertainties still persist about the origin of this style of Au-Ag-Cu mineralization, due in large part to their complex tectono-metamorphic history.

The objective of the current visit is to examine the local geology of the deposit and to illustrate the effects of deformation and metamorphism on gold-bearing polymetallic assemblages. Careful examination of the ore demonstrates that the remobilization textures and structures are related to numerous episodes of deformation of the deposit and its host rocks. A recent study by Teasdale et al. (in prep.) demonstrates that metamorphic remobilization of in situ Au-Ag-Cu-rich protore can account for the development of significant portions of the structurally-controlled gold mineralization.

Regional setting

The geology of the Cadillac mining district and its enclosing gold deposits has been described in detail by Tourigny et al. (1988, 1989a, 1989b, 1993) and Marquis et al. (1990a, 1990b).

The Cadillac mining area is located in the southeastern part of the Abitibi greenstone belt (Fig. 1). Supracrustal rocks of the district consist of a typical volcano-sedimentary assemblage composed of polydeformed mafic to felsic volcanic and volcaniclastic rocks flanked by narrow clastic sedimentary units (Tourigny et al., 1988; 1989a, 1989b; Stone, 1990). The volcanic and sedimentary rocks strike east-west to northwest-southeast and dip steeply south, parallel to the regional schistosity.

Along with the Bousquet #1, Dumagami and Doyon deposits, Bousquet #2 occurs within a zone of intense ductile-brittle deformation known as the Dumagami Structural Zone (DSZ; Tourigny, 1991). The DSZ is up to 500 m in width and is composed of several metre-scale anastomosing shear zones easily recognizable by intense transposition, hydrothermal alteration and veining of the adjacent lithologies. The highest grade of regional metamorphism in the mine area is transitional between greenschist and amphibolite facies, as represented by the hornblende-oligoclase-biotite-clinozoisite assemblage in mafic metavolcanic rocks (Stone, 1988; Tourigny et al., 1989a). In the mineralized fault zones and subsidiary fractures, retrograde metamorphism ranging down to the lower greenschist facies is expressed by pervasive replacement of prograde assemblages (Tourigny et al., 1989b). Rock types underlying the Bousquet #2 property include a variety of schist and fault rocks (cf. Sibson, 1977) derived from mafic to felsic volcanic and volcaniclastic rocks of the Blake River Group. Lithological contacts dip steeply south and strike east-west, parallel to the regional schistosity.

The orebodies consist of foliation-parallel massive and semi-massive pyritic lenses and pyritic breccias located within a metamorphosed argillic alteration zone represented by a thick unit of andalusite schist (Fig. 2). The rock is composed mainly of quartz, muscovite, andalusite (~ 5 to 25 %) and pyrite. During retrograde metamorphism, andalusite crystals were commonly pseudomorphed by muscovite, kaolinite, pyrophyllite, quartz and diaspore. Kyanite coexists locally with andalusite. The structural footwall of the deposit is characterized by the passage from quartz-sericite schist (> 50 m) to quartz-sericite-andalusite schists (20-30 m) towards the Main Sulphide

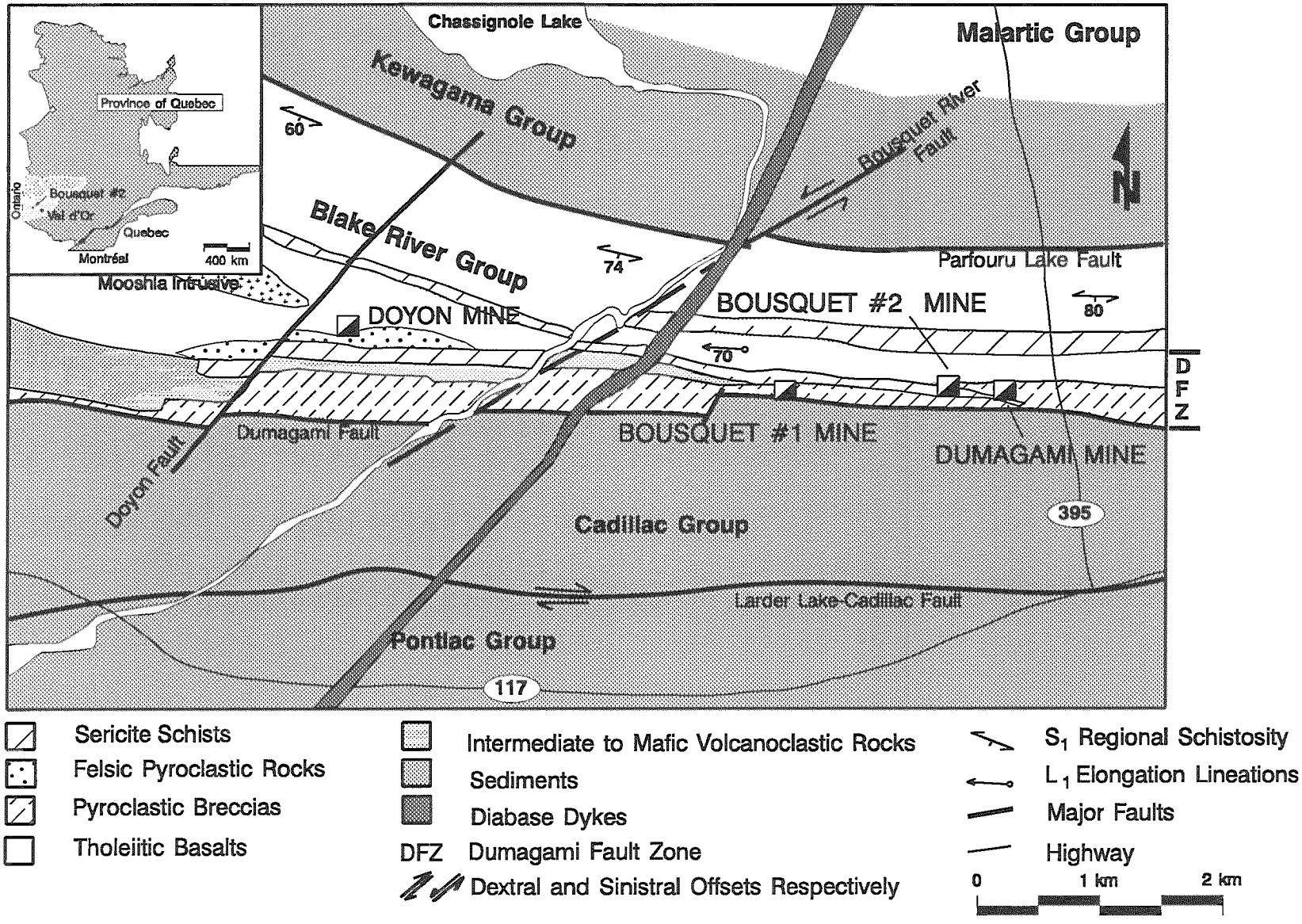

Figure 1. Simplified regional geology of the Bousquet gold district. Redrawn from Savoie et al., (1988).

Zone (MSZ). The immediate structural footwall of the MSZ, below the central part of the deposit, consists of a highly silicified and brecciated meta-rhyolite and is termed the Footwall Breccia Zone (FWBZ). This zone is interpreted to represent the underlying footwall feeder zone characteristic of volcanogenic massive sulphide deposits (cf. Sangster, 1972; Large, 1977; Franklin et al., 1981; Lydon, 1984). The quartz-sericite-andalusite assemblage is also characteristic of the structural hanging wall but is of significantly less importance here in terms of thickness (3-10 m).

Local structural setting

The most prominent structural feature of the host rocks and of the gold-bearing pyritic lenses is a penetrative, east/west-trending, steeply south-dipping (70-85°) regional schistosity (S_1). A distinct mineral-stretching lineation (L_1) is contained within S_1 and plunges up to 70° towards the west. These structural fabrics are the products of a regional deformational episode D1.

Two principal east/west-trending, subvertical ductile fault zones bound the deposit to the north and south (Fig. 2). They consist of 1 to 30 meter-wide high-strain domains that have vertical and lateral dimensions of up to 1000 m and lie along lithological contacts and at the contacts between the massive pyrite bodies and their host rocks. The inherited schistosity within these fault zones has the same strike as the associated faults, and dips steeply south (~ 70° to 80°). The schistosity commonly describes a sigmoidal pattern in cross-section. A mineral-stretching lineation plunging steeply west (> 60°) is commonly observed in foliation planes. The linear fabric and the geometry of the internal schistosity clearly indicate that reverse subvertical displacements with minor sinistral offset occurred along these faults.

A late increment of dextral strike-slip movement occurred locally along the southern fault zone where slices of graphitic schist exhibit well developed subhorizontal slickenlines and fault steps. This transcurrent displacement is interpreted as a late reactivation of an initial reverse fault because rotated and transposed metre-scale wall-rock fragments in the sheared graphitic material show subvertical mineral lineations that are distorted by subhorizontal striations.

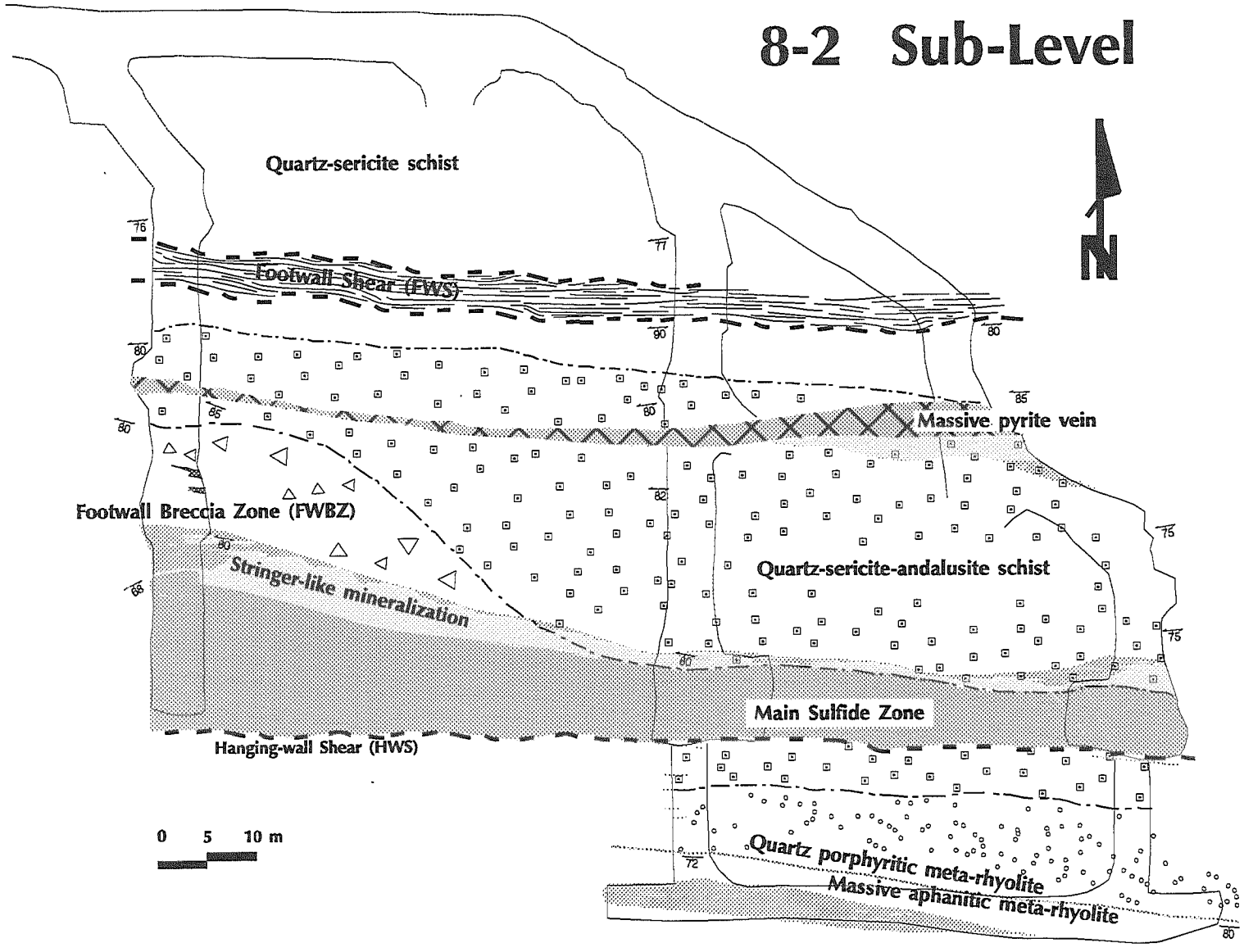

Figure 2. Geology of the 8-2 sub-level.

Sulphide facies and gold mineralization

The Bousquet #2 orebody consist of a number of pyritic zones including: 1) semi-massive to massive imbricated pyritic sub-zones defining the MSZ, 2) stringer-like and disseminated fringe zones, and 3) pyrite veins (Fig. 3).

THE MAIN SULPHIDE ZONE (MSZ)

The MSZ of the Bousquet #2 deposit consists of an assemblage of imbricated sub-zones composed of massive sulphides, sulphide matrix breccias, stringer-like mineralization and massive pyrite veins (Fig. 4). These sub-zones are distinguished by their relative sulphide contents, by their degrees of deformation, by the structural associations with their host rocks, and by their degrees of recrystallization.

Massive sulphides and sulphide matrix breccias

This type of pyritic mineralization is defined by its generally small grain size (< 1 mm) and by intense deformation. These pyritic zones exhibit a wide variety of deformational textures, including an alignment of included felsic fragments and a compositional layering parallel to S_1.

Individual sub-zones are traced laterally over distances exceeding 90 metres and are generally distinguished according to their relative sulphide contents. A consistently southward increase in sulphide concentrations is commonly observed in a large number of pyritic sub-zones (Fig. 4). This trend commonly results in the progressive passage from stringer-like mineralization (10-20% pyrite) to sulphide matrix breccia (20-80% pyrite) to massive pyrite (>80%) over distances of 1.5 to 3 metres. In numerous stopes, these asymmetric sub-zones are repeated 2 or 3 times in cross-sections measuring 3 to 5 m. The repetition of sub-zones commonly gives a cyclic appearance to the mineralization.

Sulphide-matrix breccias are characterized by felsic fragments hosted in a variably

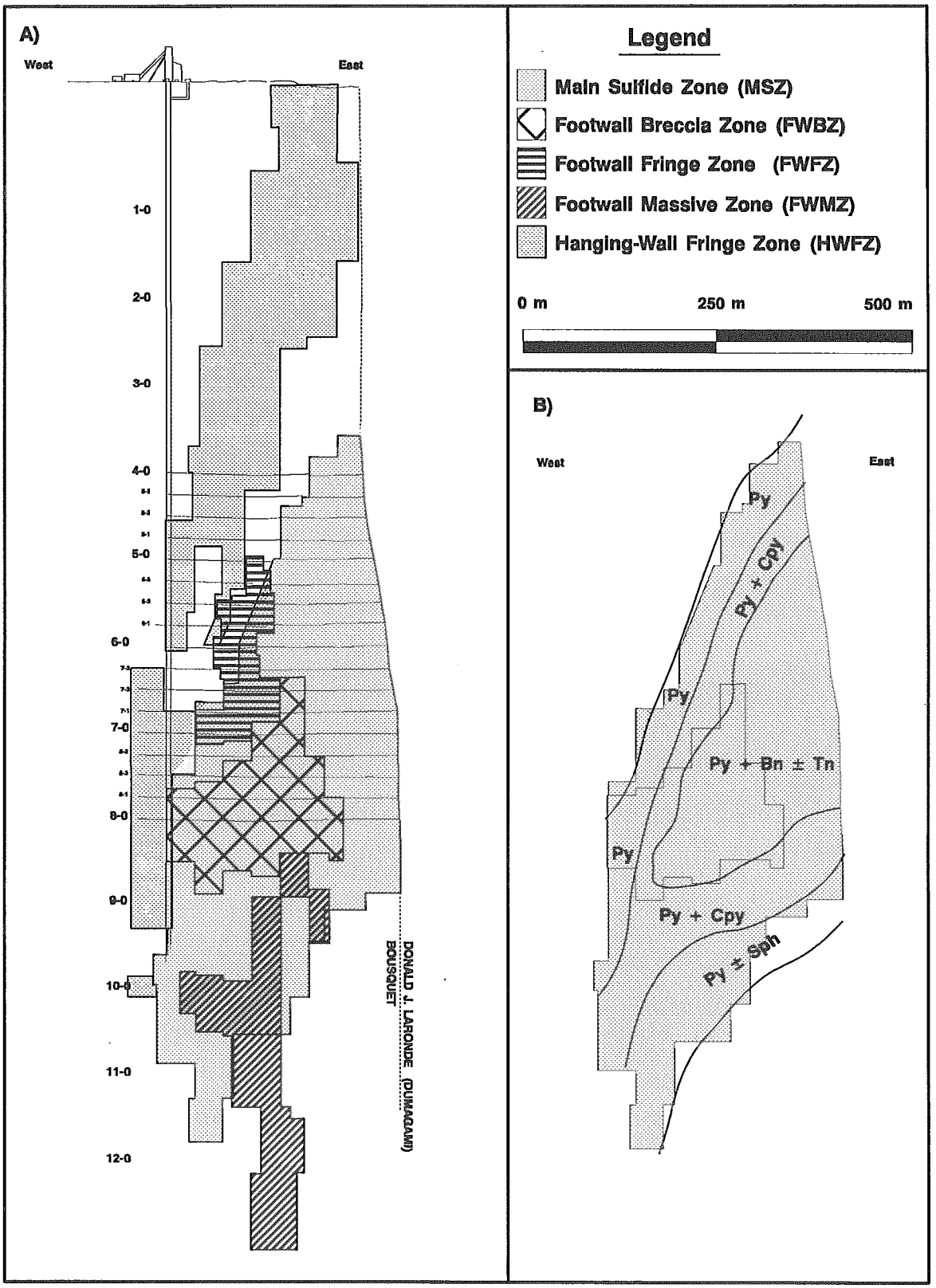

Figure 3. Longitudinal sections of the Bousquet 2 orebody. A) Mine reserves blocks, B) Schematic contours of principle ore minerals projected on the trace of the MSZ and of the FWBZ.

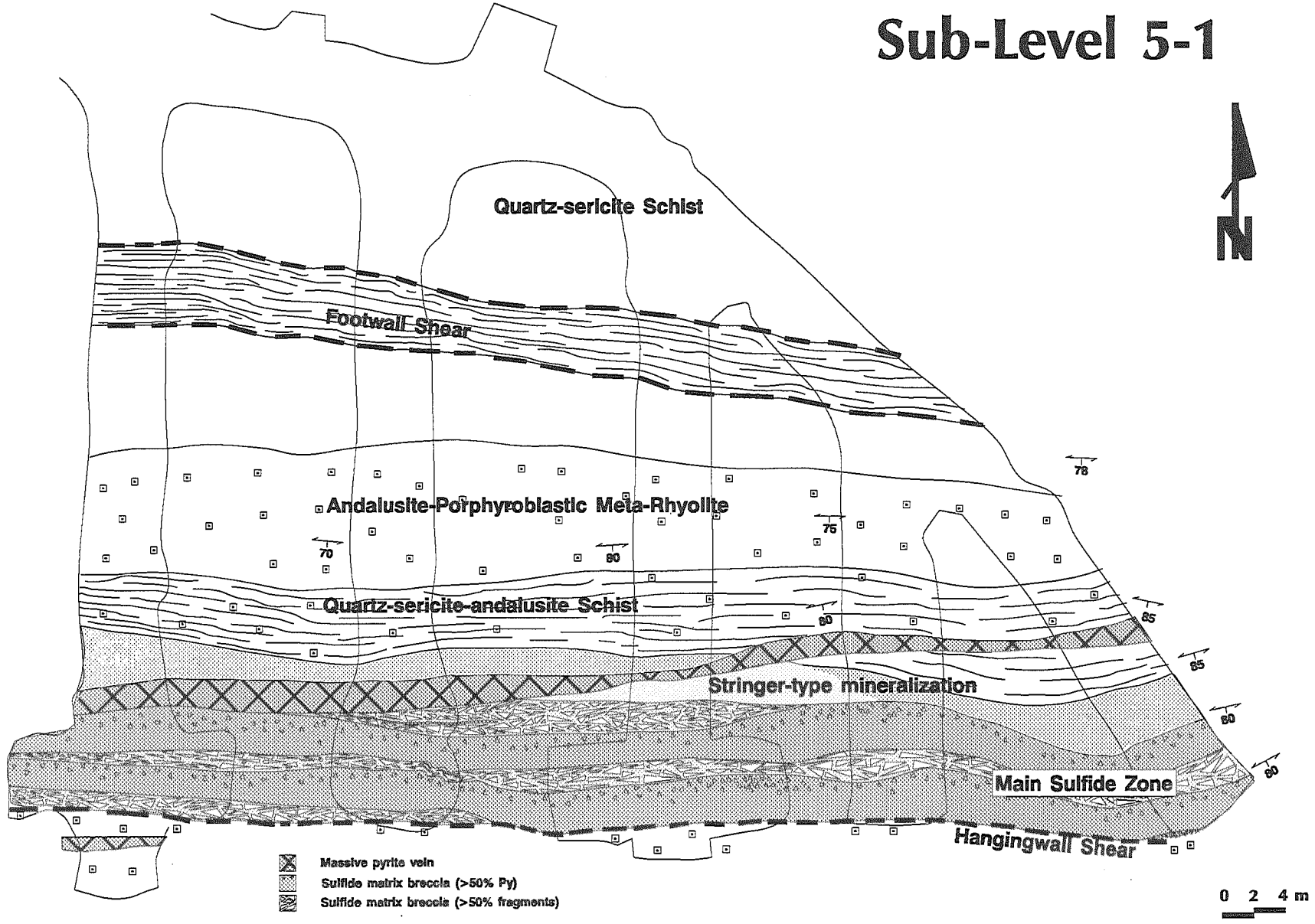

Figure 4. Geology of the 5-1 sub-level.

recrystallized pyritic matrix (20-80% pyrite ± bornite or chalcopyrite). These breccias commonly form distinct sub-zones of the MSZ or may be in progressive continuity (as described above) with stringer and/or massive zones (Fig. 4). The majority of the fragments within these breccias are foliated parallel to the regional schistosity, suggesting that a large portion of the fragmentation occurred prior to D1. This relationship is confirmed by pyrite veins which crosscut these breccias and are themselves deformed by D1.

Pyrite veins

A second type of pyritic mineralization is defined by a set of pyrite veins (>95% pyrite) showing distinct contacts with host rocks. These veins are oriented sub-parallel to S_1, yet are slightly discordant (NNE-SSW) locally, and cut across all other adjacent sulphide facies. They are characterized by well crystallized or recrystallized coarse-grained (1-3 mm) euhedral sugary pyrite and are generally less than 1 m in thickness.

These pyritic veins generally show little evidence of deformation with respect to finer grained sulphide sub-zones. This phenomenon might be the result of late annealing recrystallization which could have obliterated much of the previously imposed structural fabric and by the absence of kinematic indicators such as breccia fragments. Although few strain markers are noted in these veins, those observed confirm that these veins were emplaced during or prior to D1 (e.g., fragments elongate parallel to S_1 and dextral and inverse parasitic folding). Mapping of the 5-1 sub-level (Fig. 4) shows such a pyrite vein diverging from within the MSZ towards the northeast into stringer mineralization and further into barren quartz-sericite-andalusite schists. This crosscutting relationship clearly implies that these pyrite veins were emplaced after the finer-grained pyritic sub-zones.

Stringer-type mineralization

The structural footwall side of the MSZ, is characterized by mineralized (10-20%

pyrite) sheared meta-rhyolite (Fig. 2). This mineralization consists of foliation-parallel and slightly discordant veinlets with local accessory amounts of bornite or chalcopyrite.

Footwall breccia zone (FWBZ)

The footwall breccia zone is characterized by a highly siliceous matrix, interstitial to lapilli-block size sub-angular meta-felsic fragments, and stockwork mineralization. These fragments include both rimmed and siliceous matrix breccia fragments within the FWBZ. The zone itself is located under the central and thickest part of the Bousquet #2 deposit (Figs. 2 & 3). Mineralization within the zone consists of randomly oriented cm- to mm-size pyrite ± bornite veinlets. Deformation within the FWBZ is relatively weak compared to other zones and host rocks, based on weak schistosity development and on the random orientation of mineralization and fragments within the zone. Gold is distributed erratically within this zone (averaging 4.5 g/t).

Fringe zones

Two fringe zones are included within the mining reserves of the Bousquet #2 deposit (Fig. 3). The first, the hangingwall fringe zone (HWFZ), represents the lateral continuity of the MSZ on the western extremity of the deposit. This zone is characterized by stringer-like mineralization (10-20%) oriented parallel to or slightly discordant to S_1 in a competent quartz-porphyritic meta-rhyolite.

The second fringe zone of economic importance consists of a much smaller volume located in the structural footwall of the deposit (FWFZ). This zone is located some 12 m to the north of the MSZ on the west side of the deposit (Fig. 3). It is characterized by variably mineralized competent quartz-sericite-andalusite schist hosted in highly sheared quartz-sericite schists. Preliminary microprobe data suggest that gold mineralization in the FWFZ may be associated with pyrite mineralization in small micrometre-size fractures within the pyrite. This sulphide mineralization includes cm-size sulphide matrix breccias and 5-20% disseminated pyrite. The FWFZ is also characterized by an abundance of quartz veins emplaced during a number of episodes, none

of which appear to have been auriferous.

Sulphide Zoning and Gold-Copper Mineralization

Gold grades within the deposit are directly proportional to copper grades (Marquis, 1990a; Tourigny et al., 1993). The gold-copper-rich parts of the deposit (> 30 g/t Au, and 6% Cu) coincide with accessory amounts of bornite (± tennantite) mineralization in the central part of the deposit. Decreasing Au-Cu grades coincide with a mineral zonation from accessory bornite to accessory chalcopyrite mineralization towards the margins and the structural hanging wall of the deposit and finally to single-phase pyrite mineralization in the lateral margins of the deposit (Fig. 3). Sphalerite-rich zones are abundant in the hangingwall of the deposit and locally in lateral extensions of the MSZ (± pyrrhotite). Sphalerite-rich zones in the lateral extensions of the MSZ tend to be Ag-rich in the upper (Dumagami segment) of the deposit (P. Marquis, personal communication, 1992).

Gold and copper mineralization is found preferentially within subvertical N-S oriented tensional fractures as well as within intergranular sites between recrystallized pyrite (Tourigny et al., 1993). The N-S-trending tensional fractures cut across the foliation and are clearly late tectonic. These form undeformed, transgressive, en-echelon bornite- or chalcopyrite-rich veinlets spatially associated with a pervasive joint system in the sulphide facies host and form a significant portion of the gold mineralization in Bousquet #2. Mineralized veinlets are not uniformly developed in the mine and are increasingly abundant near the southern contact of the MSZ. Individual veinlets strike north-south, are subvertical, and obliquely transect the host rock, the schistosity, and the early massive and semi-massive pyritic bodies. The auriferous veins are coplanar with a systematic penetrative joint system (cf. Ramsay and Huber, 1987). Gold-bearing extension veins have small lateral and vertical dimensions and range from 2 mm to 2 cm in thickness (on average 3 mm). These late veins show no visible alteration envelopes. In many cases, the veinlets grade laterally into barren joints, suggesting that dilatant veins represent the mineralized segments of joints. They show no mesoscopic deformation structures and have clearly escaped the ductile deformation

that affected their host rocks. This late vein set probably influenced previous authors to suggest that gold and copper mineralization post-dated the massive sulphide mineralization.

Although the presence of gold in these structures suggest late-stage emplacement, other evidence suggests an early presence of gold and copper mineralization. This evidence includes:

1) The presence of gold and silver (with bornite, ± tennantite, ± tellurides) within quartz masses in direct association with remobilization structures at the interfaces between massive sulphides and host rocks; this association suggests remobilization from an internal source as opposed to a late addition from an external source (Tourigny et al., 1993). These piercement structures clearly demonstrate the importance of preferential remobilization. Typical piercement structures show the following sequence of minerals (Fig. 5) from least mobile to most mobile species, from the core to the apex: pyrite → chalcopyrite → bornite → quartz ± bornite ± tennantite ± tellurides ± galena ± sphalerite. The mineralogy of these quartz veins is directly analogous to that of the MSZ, further suggesting local remobilization.

2) The mine-scale mineralogical zonation of copper-rich accessory minerals from the centre of the deposit above the FWBZ outwards persists even though much of the copper mineralization occurs in late structures. This zonation is typical of VMS deposits (Large, 1992) and strongly suggests a possible genetic synvolcanic link between the copper mineralization and the massive pyrite mineralization.

3) The strong correlation between the gold and the copper grades suggests that the gold mineralization may be genetically linked to the much more abundant copper mineralization and therefore to the massive pyrite mineralization. This relationship is also typical of copper-associated gold-rich Australian deposits (Huston and Large, 1989).

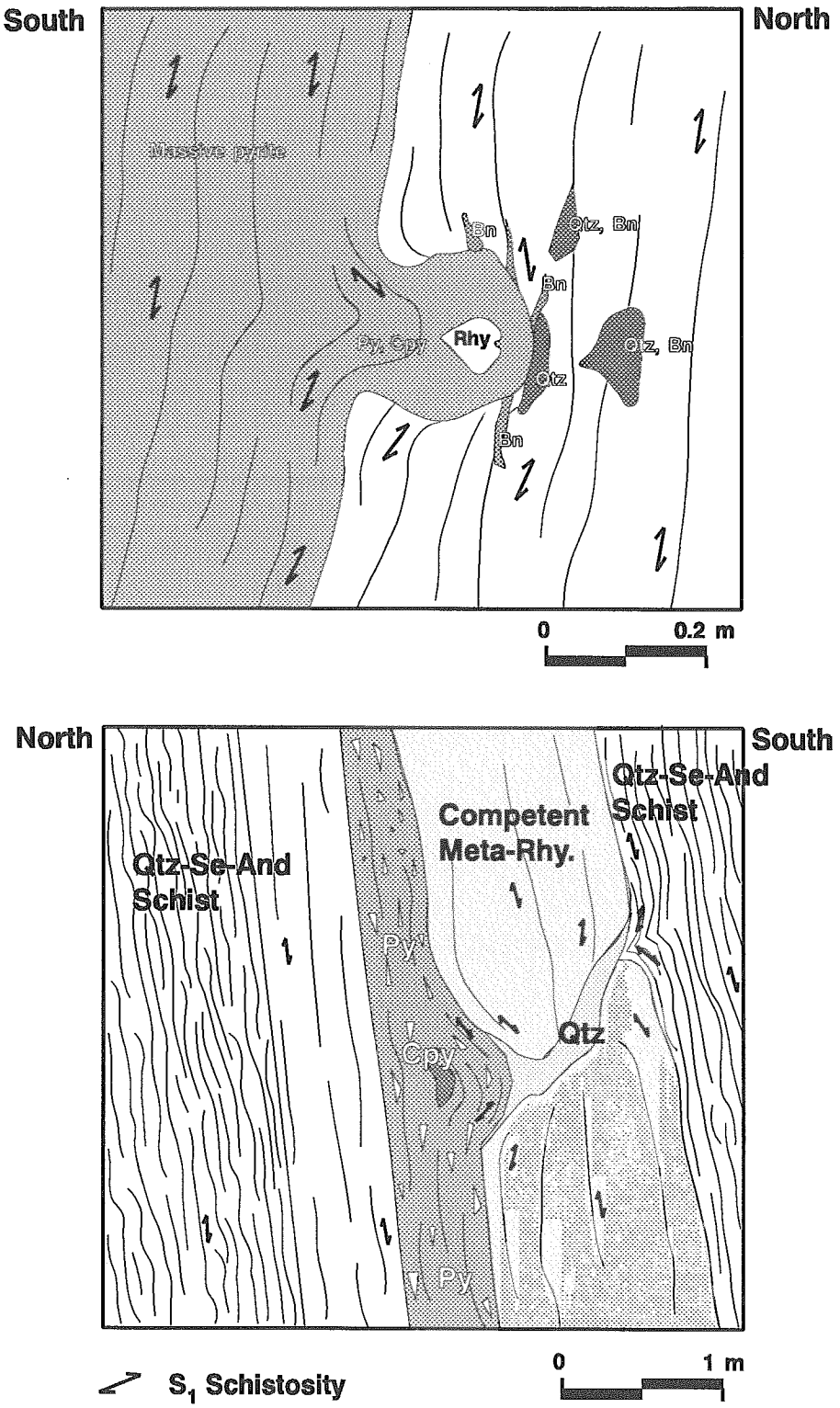

Figure 5. Line drawings from photographs of typical piercement structures.

4) The presence of visible gold mineralization oriented parallel to the foliation and having an subvertical elongation lineation parallel to L_1 suggests that gold was emplaced prior to the deformational episode D1.

These observations lead us to suggest that economic mineralization now emplaced in late structures was remobilized from an internal source as opposed to addition from an external source during late-stage deformation. As such, the Bousquet #2 deposit may represent a deformed and metamorphosed gold-rich VMS deposit of copper association similar in origin with those in Australia (Large, 1992).

Stop description

Day 1 AM

Because of the activity in the mine and frequent changes in the accessibility of underground sites, it is not possible to present in advance an itinerary for the underground visit at Bousquet #2. An intinerary will be given of the site and should include stops in the host rocks and their associated alteration zones, ductile shear zones, mesoscopic textures and structures in the pyritic orebodies, as well as local remobilization structures of sulfide-gold assemblages.

Day 1 PM

On the surface, the emphasis will be placed on the structural geology of the southern part of the Bousquet property. A large and clean outcrop will be visited within the highly deformed zone containing the auriferous mineralization.

BOUSQUET MINE PROPERTY, ZONE 6 STRIPPING AREA

Introduction

Zone 6 is an extensive sub economic Au mineralized zone occurring 200 m north of Bousquet zone 5 and 400 m north of the Bousquet zone 3 and Bousquet 2 rhyolitic horizon. Zone 6 mineralization extends for 700 m EW along the stratigraphic top of a quartz porphyritic rhyolite and is hosted mostly in the overlying basalt (Fig. 6). Most geological features characterizing the Bousquet mine economic zones are found on Zone 6 stripping. Of particular relevance to the understanding of the geological setting of the Bousquet gold deposits is the superposition of late structural and hydrothermal events on synvolcanic mineralization.

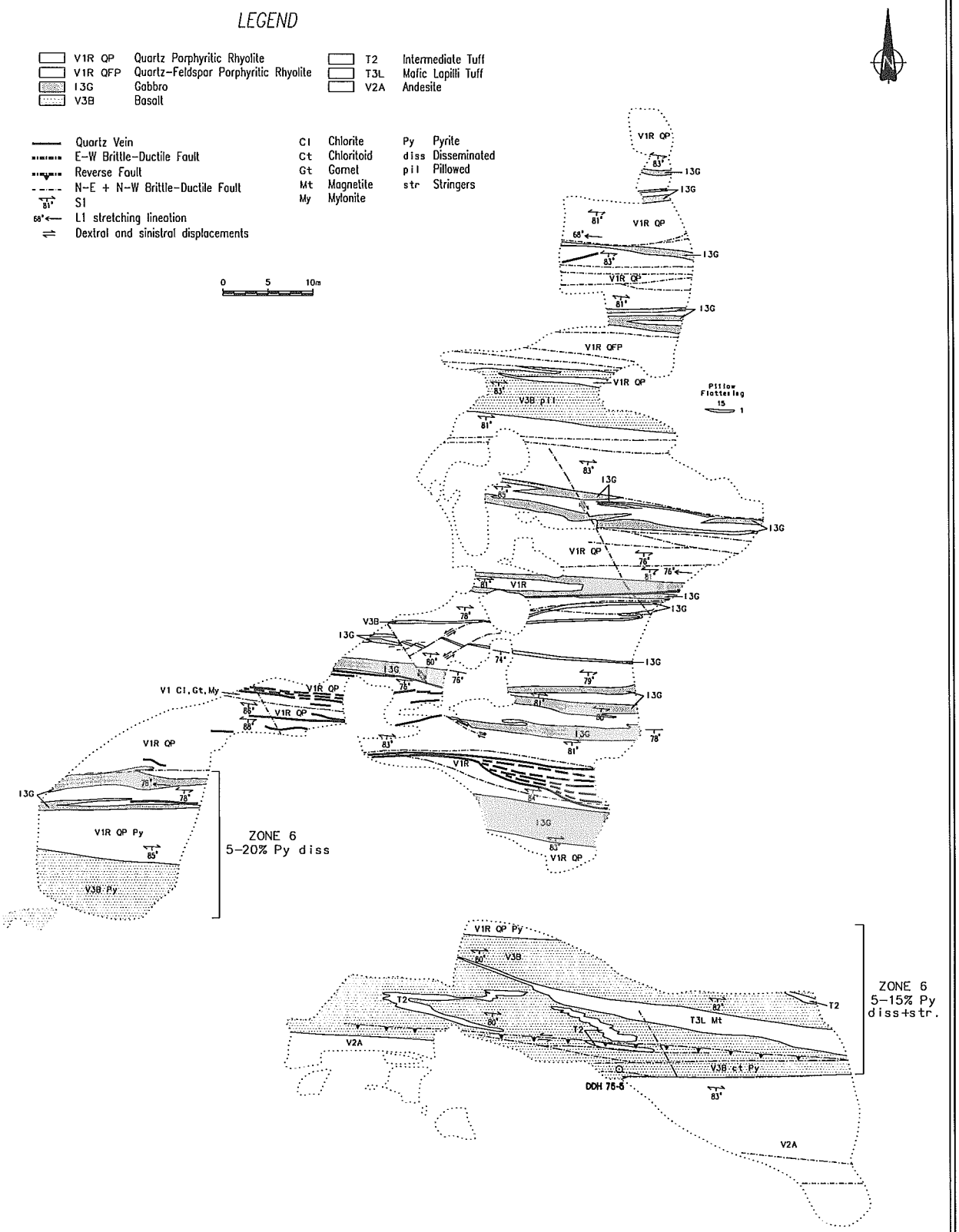

Figure 6 Geology of zone 6 stripping

Lithostratigraphic units

Quartz porphyritic rhyolite displays high strain throughout the outcrop area. Penetrative foliation, augen texture, pressure shadows around quartz phenocrysts and rotation of phenocrysts are diagnostic of the high strain state of the rhyolite. Furthermore, tectonic brecciation caused by combination of strain and hydrothermal fluid circulation is developed to various degrees throughout the rhyolite. Primary textures are mostly obliterated in this context. The rhyolite contains 5 to 15% blue quartz phenocrysts 1 to 6 mm in size throughout the outcrop zone. Variation in quartz phenocryst content being mainly a function of strain state. Hydrothermal alteration, weak at the northern end of the rhyolite increases gradually southward. Mineralogy diagnostic of this alteration gradient is the following:

1. Plagioclase phenocrysts occurring in the southern portion of the outcrop zone (5-10%) are gradually obliterated towards the top of the rhyolite.

2. Light pink syntectonic garnet porphyroblasts occur towards the rhyolite top, generally concentrated in chlorite-rich mylonitized rhyolite.

3. Sericitization increases markedly. Within the top 20 m of the rhyolite 5 to 20% coarse disseminated pyrite with minor pyrite veinlets is associated with pervasive sericitization.

Mineralized basalt overlying the rhyolite is very chloritic, vesicular and highly strained. Mineralization consists mostly of discordant pyrite veinlets (10% Py). Chloritoid porphyroblasts and magnetite are spatially associated with mineralization. Massive andesite occurs south and stratigraphically overlies mineralized basalt. Contacts between lithostratigraphic units are faulted.

Vesicular andesitic dykes cross cut the rhyolite throughout the outcrop area. These are interpreted as subvolcanic feeder dykes on the basis of their composition being identical to overlying andesite.

Structure

The penetrative S_1 schistosity ubiquitous throughout the outcrop zone is consistently oriented at N095/85°. This foliation defines a L-S fabric with stretching lineations plunging steeply westward (75°) typical of the Bousquet camp. Lithologic contacts display a consistent clockwise angular relationship with S_1. Small intermediate tuff beds locally displaying the opposite discordant relationship are tightly folded and transposed, S_1 being axial planar to fold axial trace (south of the outcrop zone, within mineralized basalt, Fig. 6).

A 10 m thick pillowed basaltic flow forms an important marker horizon in the northern part of the outcrop zone (Fig. 6). In plan view, individual pillows are highly flattened, with a long axis being oriented parallel to the S_1 foliation plane. These pillows display an axial ratio of approximately 15 to 1 in the horizontal plane. Despite this severe deformation, most of the pillows are still recognizable and indicate that this unit may be traced for over 1 km in strike length towards the east.

A conjugate set of subvertical brittle-ductile faults oriented N090° and N105° dissect the outcrop zone. These minor faults are particularly concentrated at the southern margin of the rhyolite closed to the contact with the mineralized basalt. These two sets of anastomosinf faults delimit panels of less strained rock. The faults have a reverse sense of motion which can be documented by the displacement of a small intermediate tuff unit within the southern part of the outcrop zone (Fig. 6). Quartz veins occur within these faults and are themselves deformed.

A later network of more brittle fractures is oriented at N060° and N330°. The N060° fractures have an apparent sinistral sense of motion in the horizontal plane whereas the N330° ones have a dextral sense of motion (Fig. 6). Brittle N-S fractures are also locally well developed on the outcrop zone. These brittle fractures clearly post date gold deposition. Kink bands are well developed throughout the foliated rhyolite.

Lithogeochemistry

The gradient of alteration towards the top of the rhyolite indicated by the mineralogy is confirmed

by geochemistry. Pervasive sericitization, resulting in feldspar breakdown and increase in sericite content is displayed as Ca, Na loss and K increase (Fig. 7). Chloritization is indicated by peaks in Fe and Mn.

The mineralized basaltic unit is geochemically a very distinctive unit. It is a primitive basalt (Zr=50-100 ppm, TiO2=1.0%,). This unit also displays strong hydrothermal alteration correlative with mineralogy. Magnetite and chloritoid rich mineralized zones are Na, Ca depleted and Fe enriched (25 to 33% Fe2O3). The andesite south of the mineralized basalt does not appear significantly altered (Fig. 7).

Mineralization

1. Gold occurs within two very different setting within zone 6:

   In the mineralized basaltic unit anomalous gold is associated with millimetric pyrite veinlets discordant to foliation (5-10% Py). Gold is particularly concentrated within a magnetite rich mafic lapilli tuff unit containing also 5 to 10% millimetric pyrite veinlets (up to 2.25 g/t Au over 1.6 m). This gold bearing unit is also enriched in copper (up to 750 ppm) and zinc (up to 4466 ppm) relative to the mineralized basalt. Gold displays a positive correlation with Cu and negative with Zn. This mafic lapilli tuff unit ranges from 0.5 to 3 m in thickness and can be followed for over 60 m along strike on the outcrop.

2. At the top of the QP rhyolite the zone of disseminated pyrite is anomalous in gold content.

   The best gold concentrations occur within E-W shear zones in association with quartz veining (up to 7.17 g/t Au / 1.0 m). These gold bearing sheared quartz veins are preferentially located at or close to gabbro/rhyolite contacts within the top of the rhyolite sequence. The disseminated pyrite within the QP has low base metal content (50-100 ppm Cu and Zn).

The stratabound nature of the gold mineralization within the mineralized basalt, the association of gold with base metals, and the typical VMS type alteration in the foot wall rhyolite, make a strong case for synvolcanic introduction of the gold mineralization. However, presence of gold in quartz veins within the

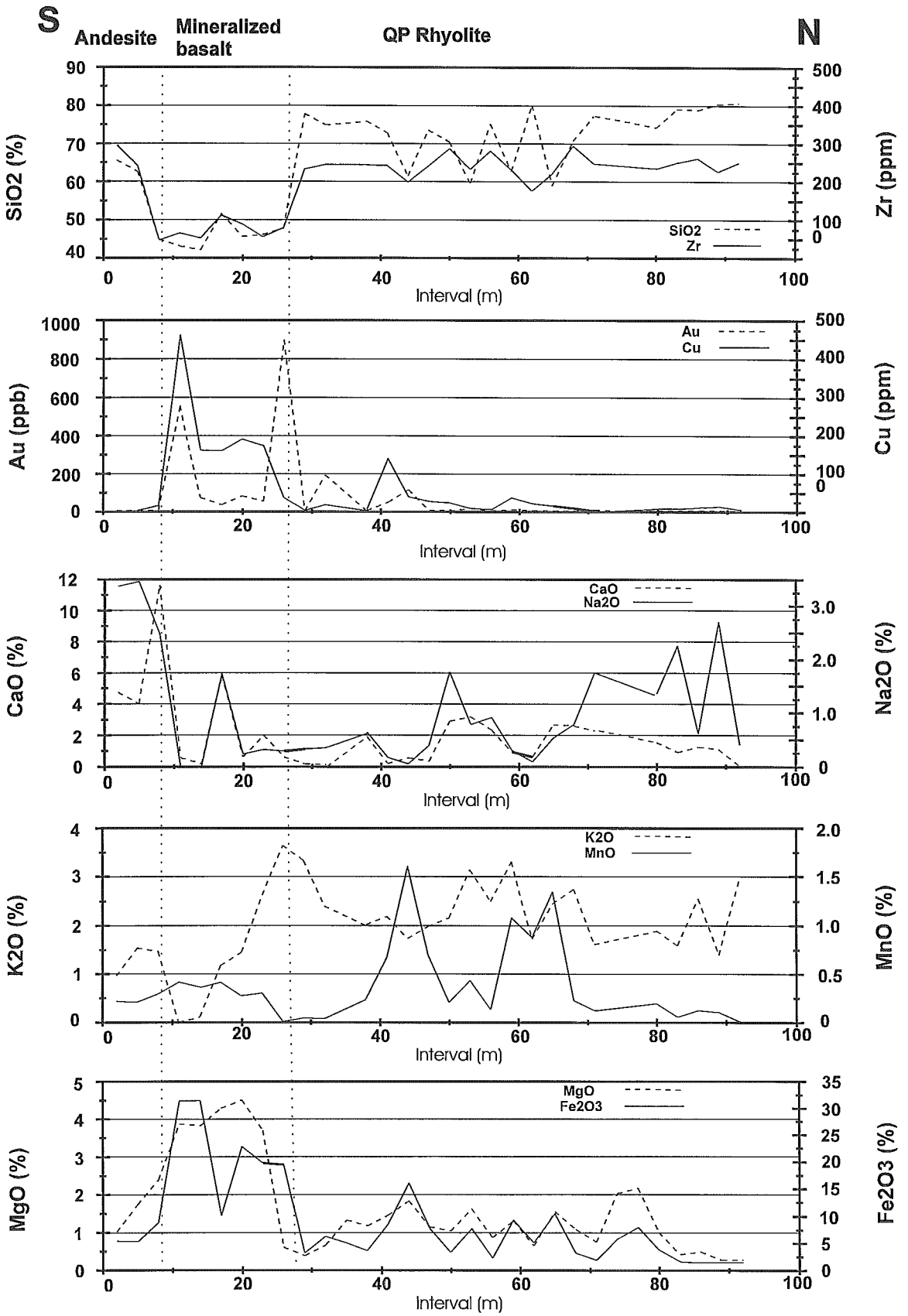

Figure 7 Geochemical profiles of zone 6, Bousquet mine property.

rhyolite indicates a structurally controlled episode of gold deposition as well. Gold occurring in quartz veins may originate from an external source or from remobilization of synvolcanic gold deposition. These two very different mineralization types occurring at zone 6 emphasize the importance of understanding timing of geological events to fully develop the potential of the Bouquet Mine property.

References

Bateman, P.W., 1984, Rock alteration at the Bousquet gold mine, Quebec: M.Sc. thesis, London, Univ. Western Ontario, 159 p.

Eliopoulos, D. G., 1983, Geochemistry and origin of the Dumagami pyritic gold deposit, Bousquet Township, Quebec: Unpub. M.Sc. thesis, London, Univ. Western Ontario, 263 p.

Franklin, J.M., Sangster, D.F., and Lydon, J.W., 1981, Volcanic-associated massive sulfide deposits. Economic Geology, 75th Anniv. v., p. 485-627.

Huston, D.L., and Large, R.R., 1989, A chemical model for the concentration of gold in volcanogenic massive sulfide deposits. Ore Geology Reviews, v. 4, p. 171-200.

Large, R.R., 1977, Chemical evolution and zonation of massive sulfide deposits in volcanic terrains. Economic Geology, Vol. 72, p. 549.

Large, R.R., 1992, Australian volcanic-hosted massive sulfide deposits: Features, styles, and genetic models. Economic Geology, v. 87, p. 471-510.

Lydon, J.W., 1984, Volcanogenic massive sulphide deposits Part 1: A descriptive model. Geoscience Canada, Vol. 11, p. 195-202.

Marquis, P., Hubert, C., Brown, A. C., and Rigg, D. V., 1990a, Overprinting of early, redistributed Fe and Pb-Zn mineralization by late-stage Au-Ag-Cu deposition at the Dumagami mine, Bousquet district, Abitibi, Quebec: Canadian. Jour. Earth Sci., v. 27, p. 1651-1671.

Marquis, P., Brown, A. C., Hubert, C., and Rigg, D. V., 1990b, Progressive alteration associated with auriferous massive sulfide bodies at the Dumagami mine, Abitibi greenstone belt, Quebec: Econ. Geol., v. 85, p. 746-764.

Ramsay, J. H., and Huber, M. I., 1987, The techniques of modern structural geology, Volume 2: Folds and fractures: Academic Press, London.

Sangster, D., 1972, Precambrian Volcanogenic Massive Sulphide Deposits in Canada a Review. Canadian Geolological Survey Paper 72-22, 44 pages.

Savoie, A., Perrault, G., and Filion, G., 1986, Geological setting of the Doyon gold deposits, Bousquet Township, Quebec: In MacDonald, A. J., ed., Proceedings of Gold 86, an International Symposium on the Geology of Gold, p. 97-107.

Sibson, R. H., 1977, Fault rocks and fault mechanisms: Jour. Geological Society, London, v. 133, p. 191-213.

Stone, W. E., 1988, Nature and significance of metamorphism in gold concentration, Bousquet township, Abitibi greenstone belt, northwest Québec: Ph.D. thesis, London, Univ. Western Ontario, 441 p.

Stone, W. E., 1990, Archean volcanism and sedimentation in the Bousquet gold

district, Abitibi greenstone belt, Quebec: Implications for stratigraphy and gold concentration: Geol. Society of America, Bull., v. 102, p. 147-158.

Tourigny, G., 1988, Géologie structurale et minéralisation aurifère à la mine Bousquet, Abitibi, Québec: Ph.D. thesis, Univ. Montréal, 244 p.

Tourigny, G., 1991, Archean volcanism and sedimentation in the Bousquet gold district, Abitibi greenstone belt, Quebec: Implications for stratigraphy and gold concentration: Alternative interpretation: Geol. Society of America, Bull., v. 103, p. 1253-1257.

Tourigny, G., Hubert, C., Brown, A. C., and Crépeau, R., 1988, Structural geology of the Blake River Group at the Bousquet mine, Abitibi, Québec: Canadian Jour. Earth Sci., v. 26, p. 157-175.

Tourigny, G., Hubert, C., Brown, A.C., and Crépeau, R., 1989a, Structural control of gold mineralization at the Bousquet mine, Abitibi, Québec: Canadian Jour. Earth Sci., v. 26, p. 157-175.

Tourigny, G., Brown, A. C., Hubert, C., and Crépeau, R., 1989b, Synvolcanic and syntectonic gold mineralization at the Bousquet mine, Abitibi greenstone belt: Econ. Geol., v. 84, p. 1875-1890.

Tourigny, G., Chartrand, F., Doucet, D., and Bourget, A., 1991, Geology of the Bousquet #2 Au-Ag-Cu deposit, Abitibi, Québec: Geol. Assoc. Canada- Mineral. Assoc. Canada, Program with Abstracts, v. 16, p. A125.

Tourigny, G., Doucet, D., and Bourget, A., 1993. Geology of the Bousquet 2 mine: An example of a deformed, gold-bearing

polymetallic sulfide deposit. Econ. Geol., v. 88, p. 1578-1597.

Valliant, R. L., 1981, The geology, stratigraphic relationships and genesis of the Bousquet gold deposit, northwest Quebec: Ph.D. thesis, London, Univ. Western Ontario, 323 p.

Valliant, R. L., Barnett, R. L., and Hodder, R. W., 1983, Aluminous rocks and its relation to gold mineralization, Bousquet mine, Quebec: Canadian Inst. Mining Metallurgy, Bull. 76, p. 811-819.

Geology of the Louvicourt massive sulphide deposit, Val d'Or district, Québec

by Ghislain Tourigny[1], Edmund Stuart[2], Peter Pelz[2], Yves Rougerie[2] and Louis Martin[2]

[1] Ministère des Ressources Naturelles du Québec, Service Géologique du Nord-Ouest, 400 blv. Lamaque, Val-d'Or (Québec), Canada, J9P 3L4

[2] Louvicourt Mine, 5999, 3e Avenue Est, C.P. 2117, Val-d'Or (Québec), Canada, J9P 6V2

Introduction

The Louvicourt mine is an Archean Cu-Zn-Ag-Au volcanogenic massive sulphide (VMS) deposit located in the southeastern part of the Abitibi greenstone belt approximately 25 km to the east of Val d'Or (Fig. 1). The deposit was discovered in 1989 during a deep drilling program designed to discover base metal reserves within favourable stratigraphy beneath the past producing Louvem mine (Boisvert et al., 1991). The deposit owned 30% by Aur Resources Inc., 45% by Novicourt Inc. and 25% by Teck Corporation, is currently believed to represent the down-dip and downplunging northeast extension of the Louvem No. 6 zone from which no previous production had occured. The deposit is a relatively deep orebody, the bulk of the known mineralization occuring at depths between 400 and 900 m below surface. Development of the mine began in 1992 with sinking of a 750 m exploration shaft to allow early development of the upper portion of the deposit and to provide a platform for underground definition diamond drilling. The main production shaft was sunk concurrently to a depth of 965 m and followed by construction of the concentrator and other surface facilities. As of december 1994, more than 15,000 m of underground tunneling and 130 km of underground drilling had been completed.

In April 1994, undiluted geological reserves, incorporating a 2% copper equivalent cut-off grade, were estimated at 15.7 million Tonnes grading 3.4% Cu, 2.2% Zn, 31g/T Ag, and 0.9g/T Au. Geological and geophysical data obtained from recent underground diamond drilling programs indicate that the deposit remains open down-plunge.

The purpose of this field trip is to illustrate the complex lithotectonic setting of the deposit during an underground visit devoted to typical lithologies, mineralization facies and structural features of both host rocks and massive sulphide orebodies.

Regional setting

Greenschist facies surpracrustal rocks of the Val d'Or area represent a typical volcano-sedimentary assemblage composed of mafic-ultramafic volcanic complexes overlain by andesitic to rhyolitic units flanked by clastic sedimentary rock units (Fig. 1). These volcano-sedimentary assemblages are juxtaposed along

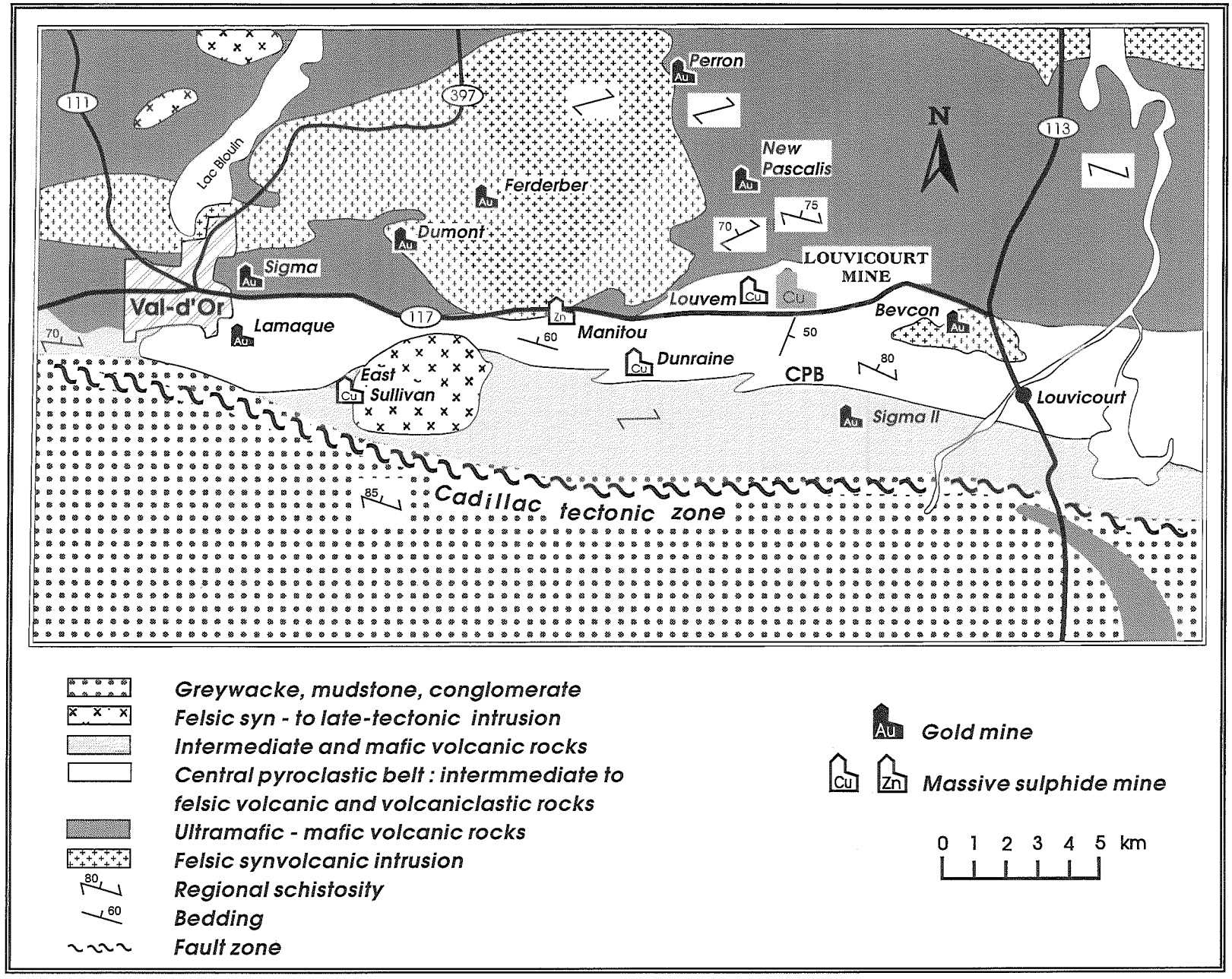

FIGURE 1. Simplified geological map of the Val-d'Or mining district and location of the Louvicourt massive sulphide deposit.

major northwest-southeast and east-west trending tectonic zones, which define tectonic blocks that are stratigraphically and structurally independant from one another (Desrochers et al., 1993).

The outstanding structural feature of the district is the presence of the Cadillac tectonic zone (CTZ of Robert, 1989) that separates the Abitibi greenstone belt to the north from the Pontiac Subprovince to the south (Fig. 1). This fault and its subsidiary deformation zones exhibit a complex kinematic history involving components of high angle reverse faulting, subvertical elongation and dextral transpression (Robert, 1989). A regional steeply dipping schistosity is variably developed and generally trends at a low angle to subparallel to major structural discontinuities. At the regional scale, lithologies strike mostly east-west, dip steeply north and are intruded by a variety of synvolcanic to late tectonic dioritic to tonalitic plutons (Fig. 1). Bedding is overturned, with younging directions facing mainly to the south. However, northeast, north-south and northwest striking strata and north- or east-facing beds have been recently observed in the volcanic strata (see Chartrand, 1991; Tourigny and Stuart, 1994). This complex structural pattern is related to the presence of both major and minor folds related to the development of the regional schistosity. Late tectonic structures overprinting S_0 and the regional schistosity occur as subvertical NE and NW trending conjugate kink bands. The kink bands have no influence on the internal stratigraphy of the volcano-sedimentary assemblage and only slightly distort previously developed planar and linear structures.

The Louvicourt VMS deposit is situated approximately 7 km north of the CTZ in the southern part of the Malartic Group (Latulippe, 1976). In this area, the Malartic Group includes effusive rocks ranging from basaltic to rhyolitic in composition with associated volcaniclastic rocks. Of metallogenic interest is the Central Pyroclastic Belt (CPB), a band of abundant volcaniclastic rocks intercalated with effusive strata and mafic sills (Sharp, 1968; Chartrand, 1991). The CPB is the host to several Cu-Zn VMS occurences including the Louvicourt mine and four past producing mines: the East Sullivan, Golden Manitou, Dunraine and Louvem Mines. The host rocks for these deposits are mostly explosive in origin and range from tuff breccia to lapillistone to ash tuff (Chartrand, 1991). The CPB extends from just west of Val d'Or to the east of Louvicourt village. It is composed of approximately 50 % of andesitic to rhyolitic pyroclastic rocks, 45

% of andesitic to rhyolitic lava, 5 % intrusive sills and minor chemical sediments (Chartrand, 1991).

Property geology

The Louvicourt VMS deposit is situated on the Louvex-Louvicourt property which is located in the northern part of the CPB (Fig. 1). The former Louvem mine Cu-Zn orebodies, which account for past production of 1.07 millions tons of ore grading 1.95 % Cu as well as 0.83 million tons of ore grading 0.19 % Cu, 8.47 % Zn, 47 g/t Ag and 1.7 g/t Au (Raymond, 1983), lie immediately to the west of the Louvicourt property.

Due to the scarcity of good surface exposures, the geology of the property has been largely elucidated by drill-hole interpretation and by underground mapping at the Louvem and Louvicourt mines.

The rocks on the Louvex-Louvicourt property are divided into three lithotectonic domains on the basis of their coherent stratigraphy and characteristic deformation features (Fig. 2). These domains are juxtaposed along major ENE-trending subvertical faults (Fig. 2).

The Northern domain occupies the northern part of the property and contains a relatively undeformed zone forming a south-facing homoclinal stratigraphic succession. Lithologies are mainly composed of massive, pillowed and brecciated andesitic flows that exhibit good lateral continuity. All lithologies in this domain strike east-north-east and dip steeply north, parallel to the regional schistosity (Fig. 2). Well-preserved primary features, such as pillow configurations, clearly indicate a constant southward-facing direction and reveal that the stratigraphic succession is overturned (J.P. Desrochers, pers. comm., 1995).

The Central domain is separated from the adjacent northern and southern domains by two major anastomosing faults (Fig. 2). This area, which hosts the major Cu-Zn occurences of the property, represents a complexly deformed and folded lozenge-shaped block mainly composed of rhyodacitic and rhyolitic flows and intermediate to felsic volcaniclastic rocks with minor exhalative sedimentary rocks and epiclastic sediments (Fig. 2). Recent structural analysis reveals that two superposed folding events are largely responsible for the spatial distribution and internal geometry of rock units and Cu-Zn occurences

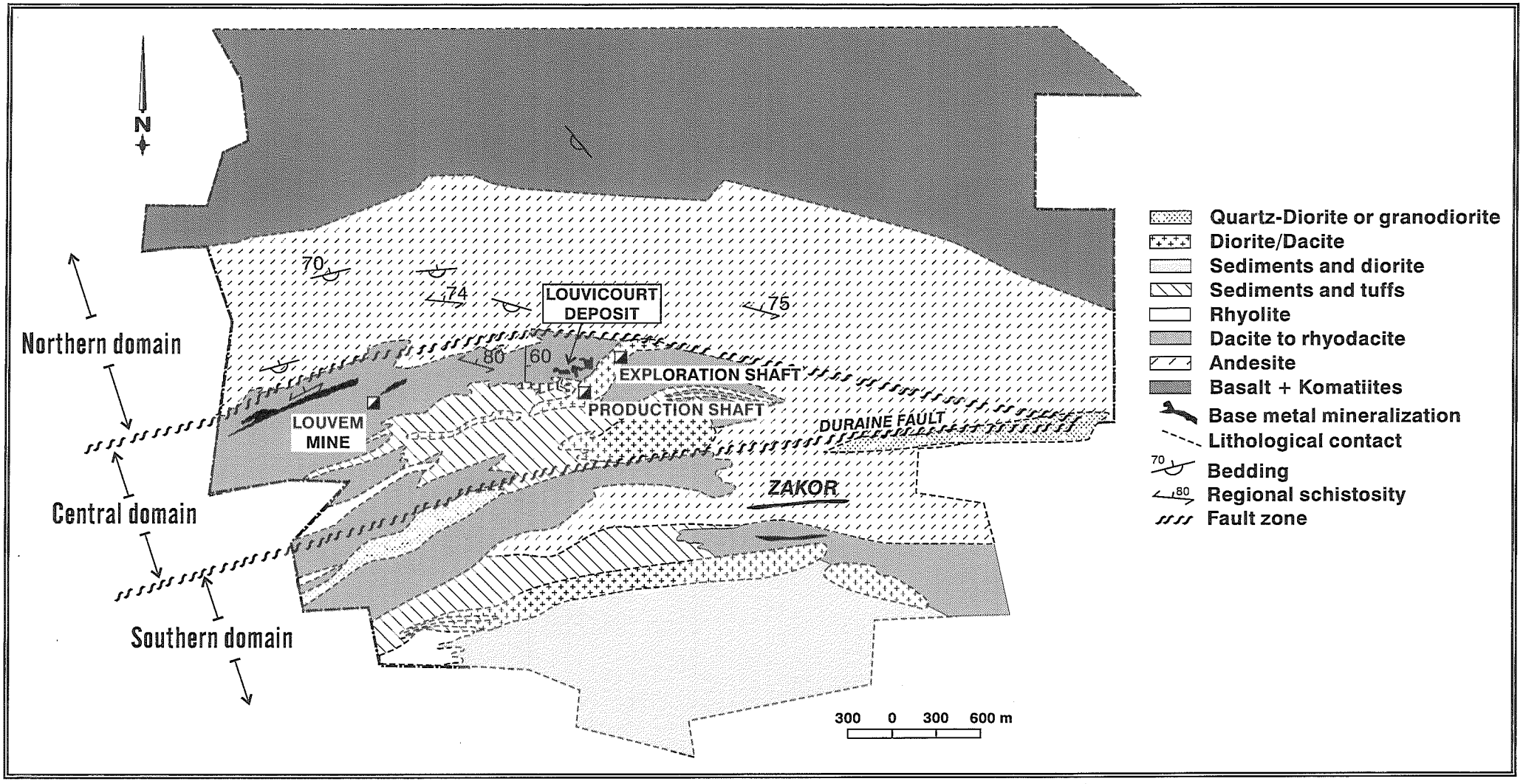

FIGURE 2. Preliminary geology of the Louvicourt-Louvex property and locations of massive sulphide occurrences.

of the domain. The interference of the two fold systems has resulted in a highly variable attitude of lithologies (Tourigny and Stuart, 1994). For example, north-south to northeast-southwest-trending bedding as well as east-facing and southeast-facing beds are identified in the mineralized volcaniclastic rock units.

To the south of the Dunraine fault, the Southern domain consists of a predominantly mixed mafic-intermediate tuff succession which attains a thickness of approximately 500 meters (Boisvert, 1993). A 160-m thick sequence of mixed intermediate to felsic volcaniclastic rocks intercalated with rare siltstone, mudstone and chert is juxtaposed against the mafic-intermediate unit to the south and east close to the Zakor sulphide showing (Fig. 2). Lithologies in this domain strike east-northeast and dip moderately to the north (50-70°). No reliable younging criteria have yet been identified in these rocks and lithological units are characterized by rapid thinning and interdigitation. Because of the highly contrasting rheological properties of lithologies and their discontinuous nature, it is most likely that the interdigitations are tectonic in origin. Tectonic layering of this type is generally the result of transposition in zones where the bedding surfaces and the predominant foliation are at a high angle to one another.

A variety of intermediate to felsic dykes and sills composed of homogeneous dark gray dacite, dark gray feldspar porphyry and light to dark gray quartz-feldspar porphyry are recognized within and adjacent to the Dunraine Fault Zone. This deformation zone, consisting of a 50 to 200 meters wide shear zone, is also characterized by abundant sericite-carbonate schist bands and local fault gouge (G. Boisvert, pers. comm., 1995).

Deposit geology

Lithologies

The Louvicourt deposit is a Cu-Zn-Ag-Au deposit occuring within a volcano-sedimentary sequence composed of volcaniclastic rocks and associated epiclastic sediments (Fig. 3). This volcano-sedimentary sequence forms a sedimentary wedge, ranging in apparent thickness from 30 m to more than 200 m in places (Stuart et al., 1994). The sulphide mineralization overlies a felsic volcanic sequence composed of rhyodacitic to rhyolitic flows intercalated with fragmental felsic rocks (Fig. 3).

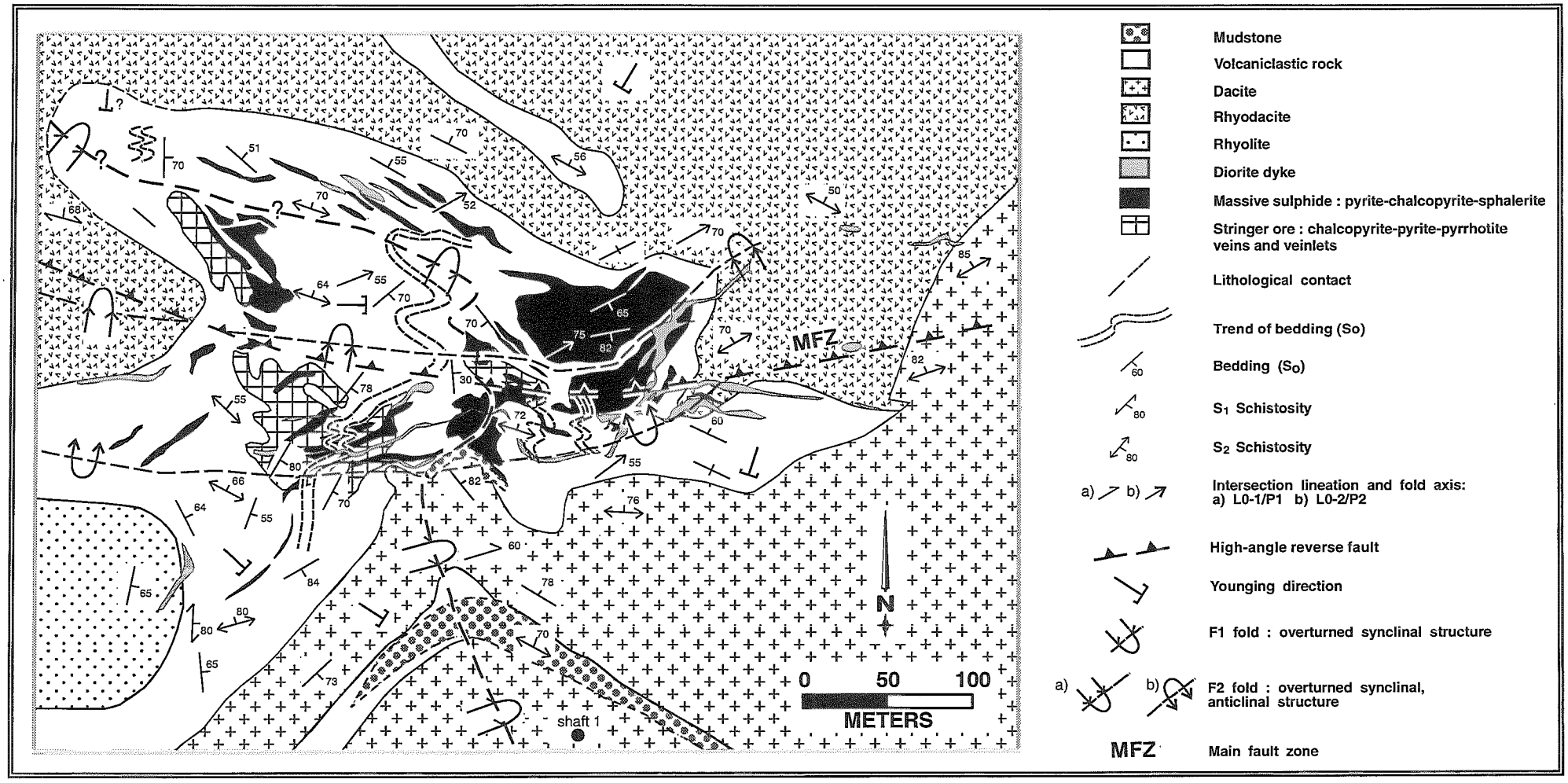

FIGURE 3. Geology and structural interpretation of the 655 level, Louvicourt mine.

The *immediate stratigraphic footwall* of the orebody consists of coarse monolithologic rhyodacitic flow breccia. This fragmental unit is distinguished by the presence of 5 to 25 % white, siliceous aphyric fragments. Individual fragments range from 1 cm to more than 1 m in size, are subangular to subrounded and are composed of subhedral resorbed feldspar crystals, quartz and sericite with minor chlorite, biotite and carbonate. The matrix is a mixture of very fine grained quartz and plagioclase with subordinate muscovite and chlorite laths aligned parallel to the dominant foliation. Accessory minerals are represented by chloritoid, rutile, carbonate, epidote, apatite, tourmaline and biotite porphyroblasts. Foliation-parallel and foliation-oblique quartz veinlets are common in this unit.

The *principal sulphide-host rocks* consist of a volcano-sedimentary sequence composed of alternating coarse and fine grained tuffs, exhalative chert and pyritic mudstone. Most of these rocks consist of varying proportions of quartz, feldspar, muscovite, chlorite, carbonate and pyrite. Accessory minerals include epidote, leucoxene, sphene, rutile, tourmaline, magnetite and garnet. The sequence commonly fines upward from coarse grained tuff at the base to pyritic mudstone at the top, and is capped by a large sub-conformable dacitic dyke.

The lower part of the sequence comprises coarse lapilli tuffs containing mainly rhyodacitic clasts (Stuart et al., 1994). The lithic fragments (mm to cm-scale) are subangular to ovoid in shape and are composed of plagioclase, quartz and sulphides. Most of them have been strongly altered to carbonate and white mica ± chlorite ± epidote. The groundmass is a mixture of recrystallized quartz, sericite and chlorite. Layers range in thickness from 1 cm to 1 m. Well developed normal graded bedding occurs in some layers and clearly indicates an east to southeast younging direction for the local stratigraphic sequence (Fig. 3).

The fine grained tuff is a well-sorted light to dark gray sericitized fine-ash tuff. These layers generally overly the coarse grained tuff but some may be intercalated within the lower strata. The rock is composed of minor vitric fragments with rare quartz and feldspar phenocrysts embayed in a sericitized fine ash matrix. The vitric fragments have a shard-like morphology and have been altered to a mixture of sericite and chlorite: they may represent altered pumice.

Exhalative chert units are characterized by dense gray cryptocrystalline silica layers up to 1 cm in

thickness with sparse muscovite partings. The chert commonly contains up to 10 % disseminated pyrite and sphalerite with bedding-parallel pyrite veinlets.

Pyritic mudstone layers occur mainly in the upper part of the mineralized sequence. They are very fine grained, dark gray and consist mainly of sericite (50-70 %), microcrystalline quartz (10-20 %) and disseminated to fine dusty pyrite (5-20 %).

The *immediate stratigraphic hangingwall* is a fragmental unit consisting of an heterolithic poorly sorted massive debris flow. This unit ranges in thickness from 5 to 40 m and is composed of subangular siliceous white fragments, massive sulphide fragments composed of pyrite or pyrite-sphalerite, and occasional layered tuffaceous clasts. Most of the pyroclasts are greater than 64 mm in diameter and are supported by a coarse grained matrix of rhyolitic affinity.

The mine sequence is intruded by a 150 m-thick subconformable aphyric dacite to the east and south (Fig. 3). This dark gray rock is characterized by the presence of abundant quartz-calcite amygdules which range from 1 to 30 cm in diameter. The dacite body defines a large folded structure with northeast and northwest striking limbs which are obliquely cut by the regional schistosity (Fig. 3). This crosscutting relationship clearly indicates that the dacite was emplaced and deformed before the regional deformation.

A number of late narrow mafic to intermediate dykes cut both the volcano-sedimentary sequence and the dacite. The dykes strike from east-west to northeast-southwest and dip 65-75° to the north and northwest. Their average thickness is about 2 m and some can be traced for as much as 300 m along strike and down dip.

Ore facies

The Louvicourt deposit consists of a stratabound orebody comprising two principal sulphide facies: (1) discordant stringer ore and (2) massive to semi-massive sulphides (Fig. 3).

Most of the stringer ore occupies the western and northwestern part of the orebody and accounts for approximately 20% of the economic mineralization (Stuart et al., 1994). It is composed of approximately 20 to 35% discordant cm to metre-scale chalcopyrite veins and veinlets. This mineralization obliquely

transects the bedding surfaces and should represent the stratigraphic lower part of the deposit. The discordant veinlets are randomly oriented and define braided structures composed of sinuous stringers surrounding lense-shaped wall-rock fragments. Individual veins generally exhibit evidence of severe ductile deformation such as both subhorizontal and subvertical boudinage, pinch-and-swell structures, minor folding and transposed segments. These veins clearly pre-date the original development of the predominant east-west trending schistosity.

Vein fillings consist of a predominantly chalcopyrite-pyrite-pyrrhotite ± sphalerite ± magnetite ± arsenopyrite ± tellurides assemblage with minor amounts of quartz ± feldspar, carbonate, white mica and chlorite as gangue minerals. Chalcopyrite, the most prominent base metal associated with pyrite, forms coarse xenoblastic aggregates. Recrystallized pyrite occurs as subhedral to euhedral crystals and as crystalline aggregates up to 1 cm in diameter which are enclosed and partially replaced by chalcopyrite. Sphalerite is closely associated with chalcopyrite. Pyrrhotite occurs as aggregates and as fracture filling veinlets. Recrystallized pyrrhotite is characterized by a well-developed granoblastic texture and by abundant deformation twins.

Massive and semi-massive sulphide lenses are erratically distributed underground; some massive lenses are in close spatial association with the stringer ore while other lenses are isolated and appear stratigraphically overlain by the stringer mineralization (Fig. 3). This mineralization consists of 1 to 60 m-thick tabular bodies containing more than 50% sulphides mainly composed of pyrite-chalcopyrite-sphalerite. Contacts with adjacent rocks are sharp and commonly sheared. Pyrite occurs mainly as medium to coarse grained pervasively annealed crystals displaying a granoblastic polygonal texture with triple junctions near 120°. Chalcopyrite and sphalerite generally exhibit a well developed mutual boundary texture and occur along grain boundaries and fractures in pyrite. Minute dissemination of chalcopyrite in sphalerite is typical of the Zn-rich layers.

Banded sphalerite-pyrite lenses are characteristic of the eastern part of the orebody where a Zn-rich margin is thought to represent the stratigraphic upper part of the massive sulphide. In places, the banded ore represents the most highly strained part of the massive sulphide, and the internal banding is

generally parallel to the regional schistosity. Sphalerite-pyrite layers contain subhedral to euhedral pyrite grains up to 1 mm in size disseminated in a coarse-grained, subhedral sphalerite matrix plus chalcopyrite, pyrrhotite and subsidiary amounts of arsenopyrite, galena, magnetite, tellurides and gold.

Alteration assemblages

Metamorphosed alteration zones spatially related to the orebody contain typical greenschist facies mineral assemblages and exhibit a characteristic pattern typical of VMS deposits (see Franklin, 1990). Five alteration facies are differentiated on the basis of their respective mineralogy (Fig. 4).

The discordant stringer ore is contained within an envelope of pervasive black chlorite alteration which grades outward to a sericitic alteration zone (Fig. 4). The sericitic alteration is best developed in felsic volcanic rocks such as the white fragmental breccia and is locally accompanied by chloritoid and disseminated pyrite.

A small zone of carbonate alteration forms a semi-conformable band both overlying and overprinting the black chlorite facies. This unit is composed of 5 to 50% of subrounded white Mg-rich carbonate porphyroblasts contained in a black chlorite-bearing matrix. The contact between the black chlorite and carbonate alteration zones is gradational and marked by incipient carbonate aggregates. Petrographically, the transition from black-chlorite to carbonate is marked by the replacement of chlorite by carbonate.

An important zone of green Fe-rich chlorite overlies the carbonate facies and is developed in the inner part of the massive sulphide and in the upper stratigraphic level of the host volcano-sedimentary sequence (Fig. 4). This zone is interlayered with two principal garnet-green chlorite-magnetite-bearing horizons which represent metamorphosed, syn-volcanic, altered, concordant layers. The garnet-bearing rock forms 1 to 3 m thick horizons composed of 5 to 30% subidioblastic to xenoblastic garnets with lesser amounts of chlorite, carbonate, muscovite, plagioclase, magnetite, pyrite, ilmenite and rutile. Garnet poikiloblasts contain numerous inclusions of carbonate, chlorite and quartz with lesser amounts of white mica and pyrite. Small quartz, chlorite and white mica inclusions are locally elongated parallel to the host-

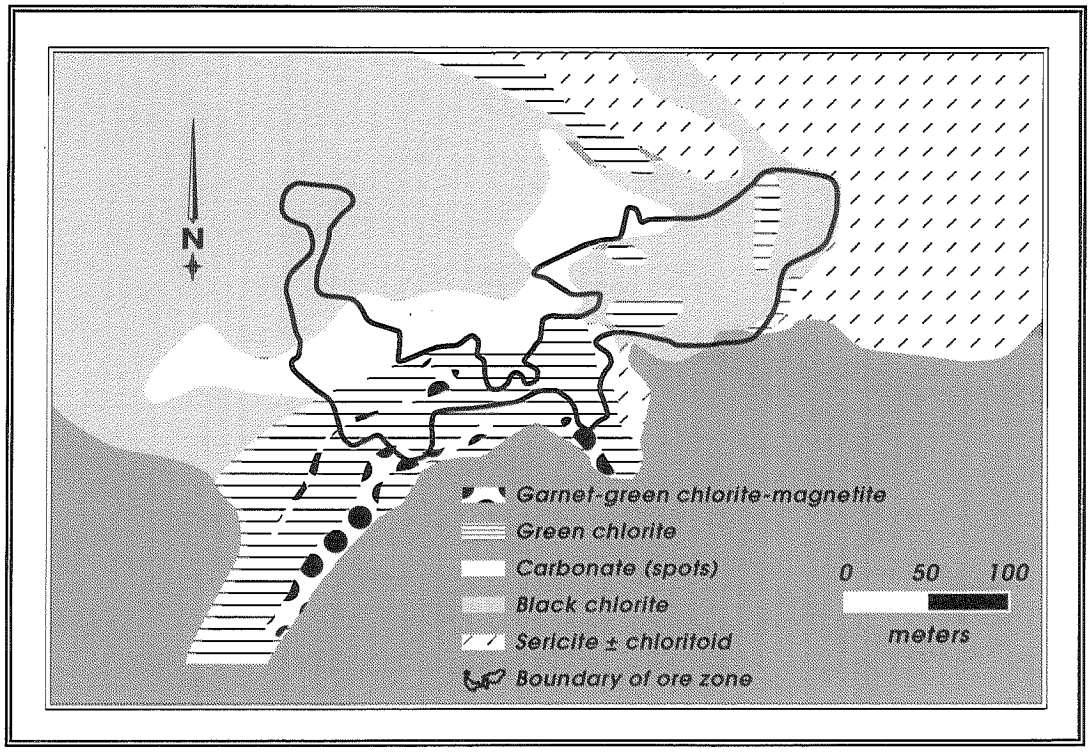

FIGURE 4. Spatial distribution of alteration facies on the 655 level, Louvicourt mine.

rock schistosity. In addition, several garnet crystals are partly replaced by carbonate and chlorite resulting in poorly developed 110, 111 and 210 faces.

Structural geology: Folds, foliations and lineations

In the immediate mine area, the volcano-sedimentary sequence and the orebody are complexly deformed and characterized by a number of planar and linear structural fabrics related to two principal generations of structures designed D_1 and D_2. As a result of these two superposed phases of folding, the attitude of the bedding surfaces (S_0) is highly variable: S_0 strikes from northeast-southwest to east-southeast-west-northwest, dips moderately southeast and north respectively and faces mostly southeast (Figs. 3 and 5).

Recent underground mapping of the 655 level has revealed the presence of a major F_1 fold affecting the immediate stratigraphic hanging wall and the adjacent volcano-sedimentary rocks (Fig. 3). Both limbs of this fold are obliquely transected by the more pervasive S_2 regional schistosity, thus clearly indicating a pre-regional (i.e. D_2) deformational origin (Robert and Poulsen, 1994).

This major F_1 fold is reclined, open and slightly overturned towards the west with a north-south trending axial surface. At the map scale, the trace of the F_1 axial surface can be traced continuously in a north-south direction throughout the deposit and its host rocks (Fig. 3). To the north side of the main fault zone (MFZ on fig. 3), the F_1 axial surface undergoes an important rotation with both S_0 and S_1 surfaces due to the presence of F_2 folds. The hinge line of the major F_1 fold has not been directly observed underground and the plunge of this fold has been calculated by determining the intersection of its two limbs. Its calculated fold axes trends 070° and plunges 60° east-northeast and is colinear with the F_2 fold axis (Figs. 3 and 5).

The S_1 foliation associated with the F_1 fold is rarely seen underground and where observed, it is usually oriented parallel to the bedding S_0 (Fig. 3). S_1 is defined by the preferred alignment of muscovite laths and oxide crystals and is commonly crenulated by the S_2 schistosity.

D_2 structural elements include a spaced cleavage S_2 and associated major and minor F_2 folds. F_2

folds are best developed in the central part of the volcano-sedimentary sequence where S_2 cuts S_0 and S_1 at a high angle. They consist of open, generally symmetrical structures, slightly overturned to the south with north-dipping axial planes. Most folded competent tuff layers have a rounded hinge morphology and typically exhibit a parallel fold geometry (class 1B of Ramsay, 1967). They vary in amplitude from cm to several m and most plunge northeast subparallel with the F_1 fold axis. The variations of the plunge and direction of the F_2 fold hinge within the S_2 surface is controlled by the initial orientation of the bedding on the limbs of the F_1 folds.

A spaced S_2 cleavage is parallel to the axial surface of the F_2 folds and has an average attitude of 280-70° (Fig. 5). It is commonly defined by the preferred orientation of ellipsoidal fragments in coarse-grained volcaniclastites. In polished thin sections, the S_2 foliation is an axial planar crenulation cleavage defined by alternating chlorite-muscovite rich septa and quartzo-feldspathic microlithons.

Mesoscopic evidence of interference patterns between F_1 and F_2 folds have been locally observed in the southwestern part of the mine, where early isoclinal F_1 folds are refolded by F_2 symmetrical buckles. Mesoscopic F_1 folds have a north-south trending axial surface and plunge steeply towards the northeast coaxial with the youngest F_2 fold axis. The interference structures are developed in interbedded chert-pyrite and chert-chloritic tuff strata. However, because no axial planar tectonic fabrics (cleavage, fracture, etc.) have been observed in the nose of the earliest F_1 flexure, and because the sulphide-chert or chert-tuff units are easily deformed, it is possible that early folds are syn-sedimentary structures (see Elliott and Williams, 1988).

Given that the F_2 fold axes seem to be parallel to the plunge of the oldest F_1 folds, the resulting map scale geometry could be similar to the type 3 interference pattern of Ramsay (see Fig. 10-13 F of Ramsay, 1967). Such an interference pattern can be seen by the trace of the refolded F_1 hinge line which seems describes an open Z-shaped geometry (Fig. 3). At the map scale, the north-south portion of the F_1 axial surface should represent the short limb of the major F_1 fold while its southern long limb would lie to the south of the property (Fig. 3). If this interpretation is correct, the spatial distribution of both lithologies and orebodies would be controlled mainly by the first phase of folding. This model requires a systematic

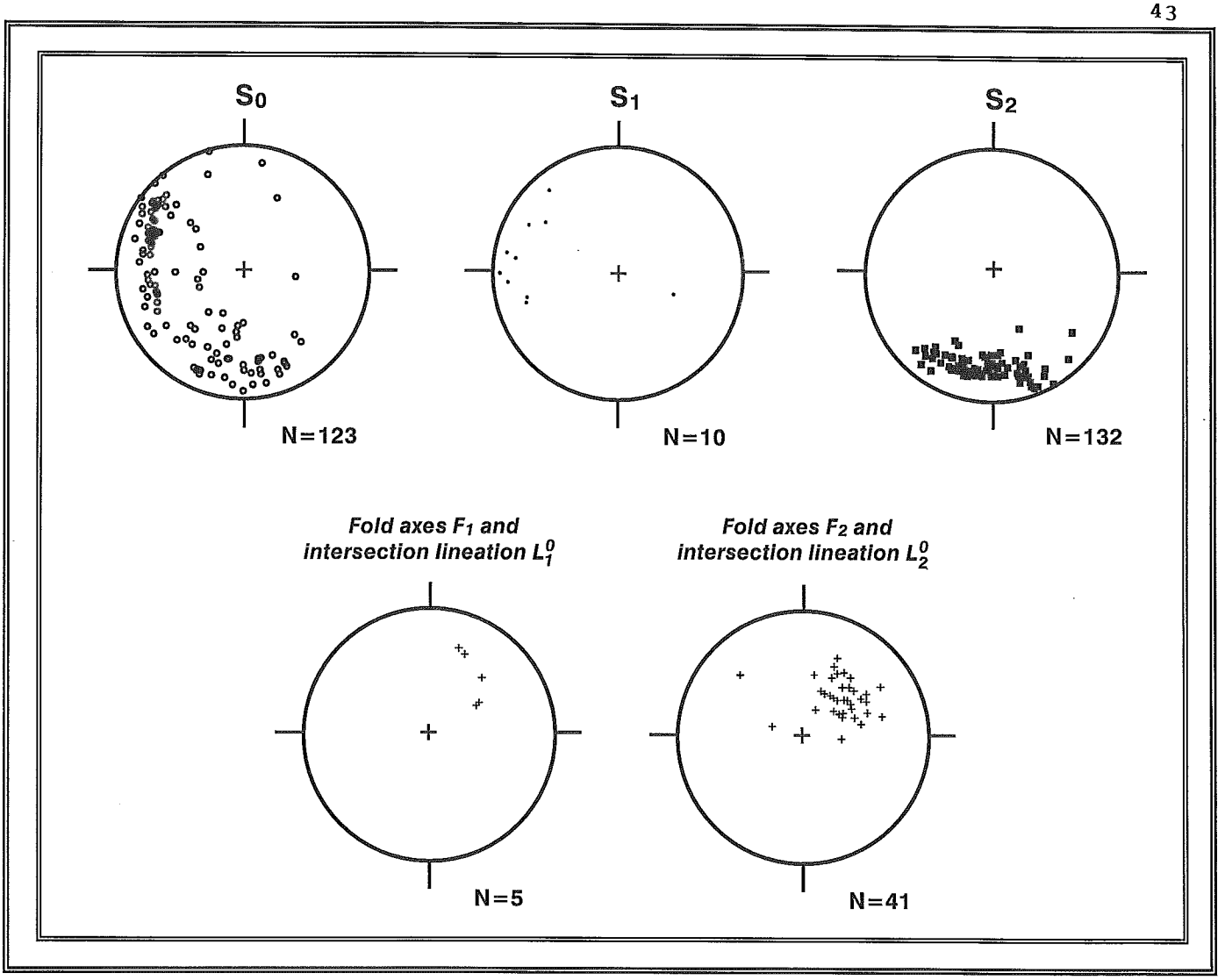

FIGURE 5. Equal-area, lower-hemisphere projections of the principal strutural elements from the Louvicourt mine.

repetition of tuff units, orefacies and metal zoning on the two limbs of the major F_1 fold. However, given that the Zn-rich part is concentrated mostly to the eastern margin while the Cu-rich stringer ore occupies the western half of the deposit, and that no reliable laterally extensive marker horizon has been identified to date, this model needs further substantiation. Alternatively, it is possible that the present axial trace of the F_1 fold separates a proximal Cu-rich ore zone from a distal Zn-rich part of a sulphide mound that had, at time of its deposition, an asymmetrical distribution of sulphide facies and minerals. Further work is necessary to resolve this metallogenic and structural problem.

Late faults and flat veins

A network of steeply north-dipping high-angle ductile faults is associated with the late increment of D_2 (Fig. 3). These faults truncate the volcano-sedimentary assemblage at a high angle but are generally subparallel or at a low angle to S_2 and F_2 axial surfaces. Fault zones vary from a few centimeters to up to 2 meters in width and have both lateral and vertical dimensions of up to 600 meters. The schistosity within these faults is the reoriented and intensified S_2 fabric. Within the fault zone, S_2 has the same strike as the overall strike of the shear, dips steeply north (60-70°), and commonly describes a sigmoidal pattern in cross section. A subvertical, down-dip mineral lineation is observed locally in S_2 planes. Combined with the geometry of the internal schistosity, this linear fabric clearly indicates a reverse sense of subvertical displacement. These faults represent an additional geometric complexity in the deposit and their influence on the ore zone morphology and distribution is not yet well understood.

Flat veins consist of undeformed subhorizontal tabular bodies occupying extension fractures developed in competent lithologies mostly along the interface between the massive sulphide bodies and the adjacent host rocks. The flat veins generally strike north-south and dip about 5-10° to the east or west. Individual veins are composed of remobilized chalcopyrite ± sphalerite ± pyrite with lesser amounts of quartz-chlorite-carbonate-white mica and native gold. They transect different lithologies as well as early formed sulphide lenses and S_2 foliation and represent the latest tectonic and hydrothermal event at the Louvicourt mine. The opening vector of the flat veins is perpendicular to the vein and given by fibrous

aggregates of quartz and phyllosilicates. This opening vector is subvertical and oriented parallel to the mineral stretching lineations measured in the host rocks: this clearly indicates that the veins formed during the subvertical elongation related to the subvertical displacement observed in the adjacent reverse fault zones.

References

Chartrand, F., 1991. Geological setting of volcanogenic massive sulfide deposits in the Central Pyroclastic Belt, Val d'Or, in Chartrand, F., ed., Geology and Gold, Rare Element, and Base Metal Mineralization of Val d'Or Area, Quebec, Society of Economic Geologist, Guidebook Series, v.9, p.75-89.

Boisvert, G., Mannard, G., Britt, C., Bubar, D. and Rougerie, Y., 1991. Geology of the Louvicourt deposit and results of the phase IV and V exploration programs. Unpublished report for Aur Resources Inc.

Desrochers, J.-P., Hubert, C., Ludden, J., and Pilote, P., 1993. Accretion of Archean oceanic plateau fragments in the Abitibi greenstone belt, Canada: Geology, v. 21, pp. 451-454.

Elliott, C.G., and Williams, P.F., 1988. Sediment slump structures: a review of diagnostic criteria and application to an example from Newfounland. Journal of Structural Geology, **10**, pp. 171-182.

Franklin, J.M., 1990. Volcanic-associated massive sulphide deposits. In Gold and Base-metal Mineralization in the Abitibi Subprovince, Canada, with emphasis on the Quebec segment: Short course notes, compiled by S.E. Ho, F. Robert and D.I. Groves. The University of Western Australia, Publication no. 24, p. 211-241.

Latulippe M., 1976. Géologie et métallogénie de l'or en Abitibi. Geological Association of Canada Annual Convention Field Excursion Guidebook, A-4 and A-2, pp. 41-53.

Ramsay, J.G., 1967. Folding and fracturing of rocks. New York, McGraw-Hill, 568 p.

Robert, F., 1989. Internal structure of the Cadillac tectonic zone southeast of Val d.Or, Abitibi greenstone belt. Canadian Journal of Earth Sciences, **26**, pp. 2661-2675.

Robert, F., 1993. Notes on the Louvicourt massive sulphide deposit. Unpublished report for Aur Resources Inc.

Robert, F., and Poulsen, H., 1994. Additional notes on the Louvicourt massive sulphide deposit. Unpublished report for Aur Resources Inc.

Sharpe, J.I., 1968. Louvicourt Township, Abitibi East County: Quebec Department of Natural Resources, Geological Report, 135, 153 p.

Stuart, E., Pelz, P., Rougerie, Y., and Martin, L., 1994. Louvicourt deposit- A first look underground. Unpublished presentation report to CIM Geological Society.

Tourigny, G. et Stuart, E., 1994. Étude structurale et métallogénique du gisement de sulfures massifs de Louvicourt. *In* Programme et résumé, Séminaire d'information sur la recherche géologique, Ministère des Ressources Naturelles du Québec, p. 39.

Geology of the Isle-Dieu Zn-Cu-Ag-Au massive sulphide deposit

Matagami mining district, Quebec

by

André Bonenfant

Noranda Mining and Exploration Inc.

Matagami Division, Matagami (Quebec), JOY 2A0

INTRODUCTION

The Isle-Dieu volcanogenic massive sulphide deposit is located in the Matagami Mining Camp of the Archean Abitibi subprovince. Mining in this camp started in 1963 and the production to the end of 1994 totals 39,285,000 metric tonnes grading 8.1 % Zn, 0.8 % Cu, 25.7 g/t Ag and 0.45 g/t Au.
Isle-Dieu, discovered in May 1985, and having the highest grade of all camp deposits, was put in production in January 1989 and will be exhausted by the end of 1997.

Noranda Mining and Exploration Inc., Matagami Division, welcomes the Precambrian'95 field trip participants and will try to present a good tour of the remaining underground exposures.

GEOLOGY

Regional Context

The Matagami mining camp is located in the north-central portion of the Abitibi Greenstone Belt, 215 km NE of Rouyn-Noranda in northwestern Quebec (Fig. 1). The deposits are located along the areally extensive Key Tuffite exhalite horizon at the contact between the Watson Lake Rhyolite and the overlying Wabassee Basalt. The volcanic sequence is intruded by a mafic igneous complex (Bell River Complex). The ensemble of rocks are folded into a large, moderately northwest plunging anticlinal structure (Galinée Anticline), its axis plunges moderately northwest. VMS are found on both flanks of the anticlines; the south flank has yield 83 % of mineral production.

South Flank Geology

The south flank deposits are associated with the Key Tuffite stratigraphic marker horizon. On the south flank the Key Tuffite has a N130°/45° attitude and has been traced over 10 km. In the area of the deposits the Key Tuffite envelopes the sulphide mounds and is subdivided into a lower tuffite and an upper tuffite.

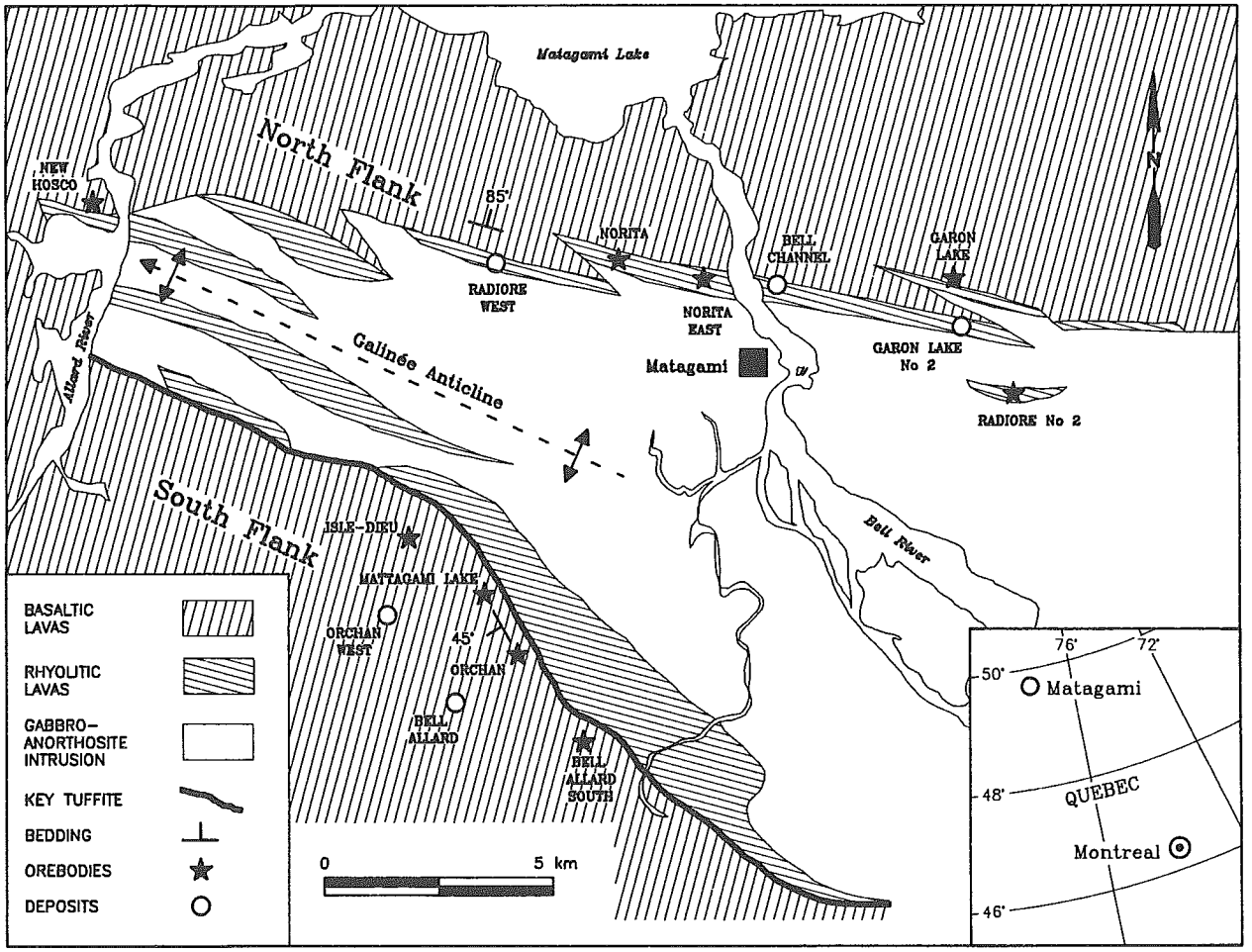

FIGURE 1 : Geological map of the Matagami area, modified from Piche (1991) and Sharpe (1968).

The deposits, made up of one or many agglomerated sulphide lenses, are distributed at approximately a 1 600 m average spacing (Fig. 2). The following deposits can be seen : Bell Allard South (235,000 t), Bell Allard (3,172,000 t), Orchan (4,514,000 t), Orchan West (< 500,000 t), Mattagami Lake (25,465,000 t) and Isle-Dieu (3,000,000 t).

Geology of the Isle-Dieu deposit

The upper part of the Isle-Dieu deposit is found at a depth of 325 m (Fig. 3). Fifteen to thirty metres of overburden covers the volcanic sequence. The upper part of the volcanic sequence is composed of basaltic lavas inclined 45° south-west and is cross-cut by two gabbro dykes varying from 75 to 150 m in thickness.

The upper and lower tuffites vary in thickness from roughly from half a m to 20 m respectively. The deposit is made up of two main sulphide lenses (Nos. 1 and 2) and two satellite masses (nos. 1C and 1D). Projected on an horizontal plane, the sulphide masses have an elliptic shape which has a WNW-ESE orientation (Fig. 4). The two main bodies are some 420 m long and have an average thickness of 25 and 10 m respectively. Tonnage for all lenses totals 3,000,000 tonnes grading 18.07 % Zn, 1.04 % Cu, 81.94 g/t Ag and 0.48 g/t Au.

Some of the sulphide bodies have been split by a 40 m thick tonalite dyke (Fig. 5).
The concordant portion of the sulphide masses forms a sulphide mound while the discordant portion, the chimney area, is constituted of many types of chimneys having varying compositions (Lavallière et al., 1992).

The lens-shaped massive sulfides are composed of 40 % red medium grained (locally yellowish) sphalerite alternating with millimetric to centimetric bands of pyrite (10 %), chalcopyrite (6 %), pyrrhotite (4 %). Chalcopyrite, pyrrhotite and magnetite (7 %) are mostly concentrated at the lenses base, in proximity to the mineralized pipes. Disseminated galena (1 %) is found in the mineralized mass along with gangue material (32 %) essentially composed of cherty residues, silica, carbonate, chlorite and talc. Individual chimneys are oriented N280°/80° and have a thickness varying from 15 cm to 5 m. These

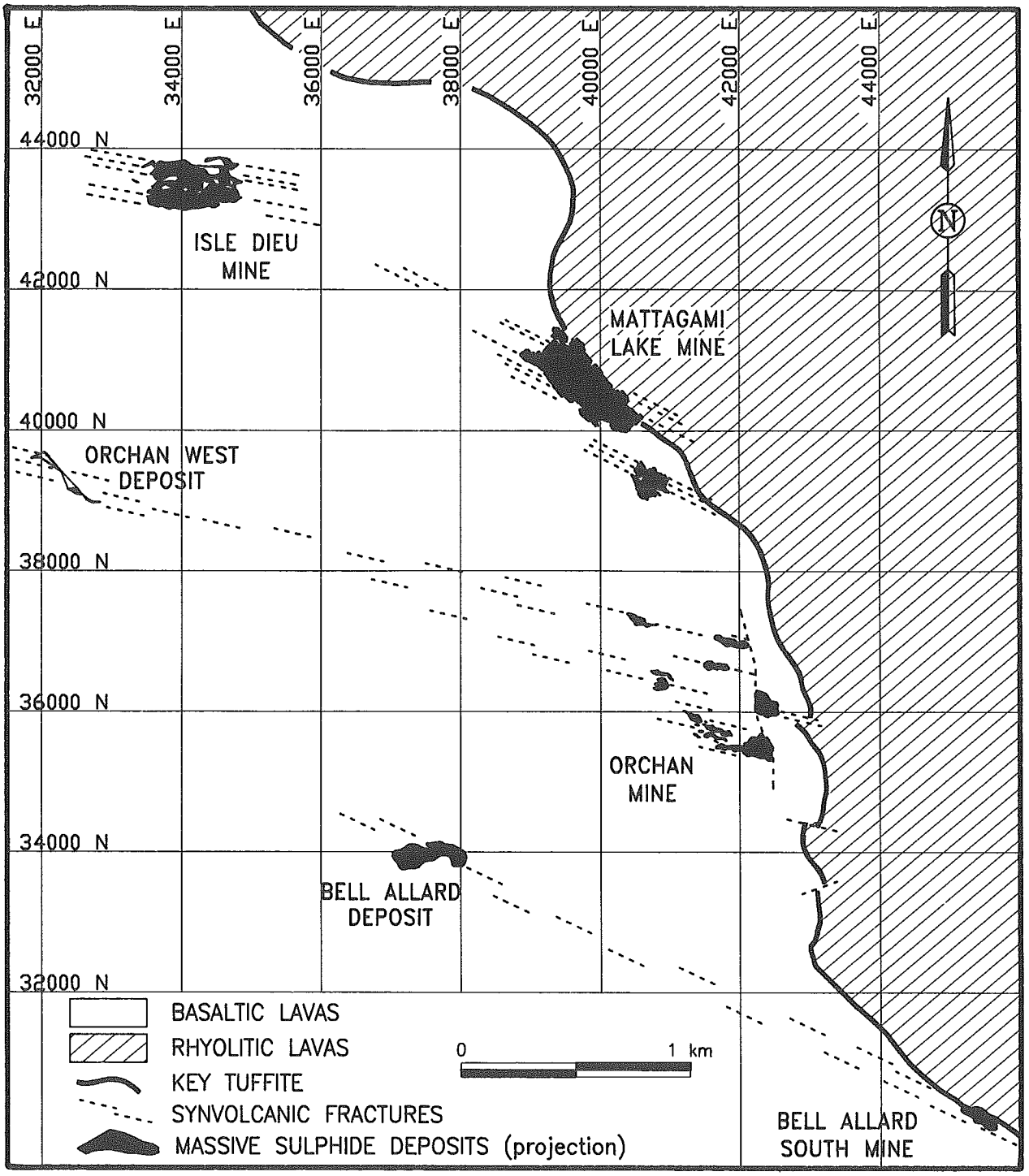

FIGURE 2 : Map showing the Galinée Anticline South Flank deposits, Matagami, Québec.

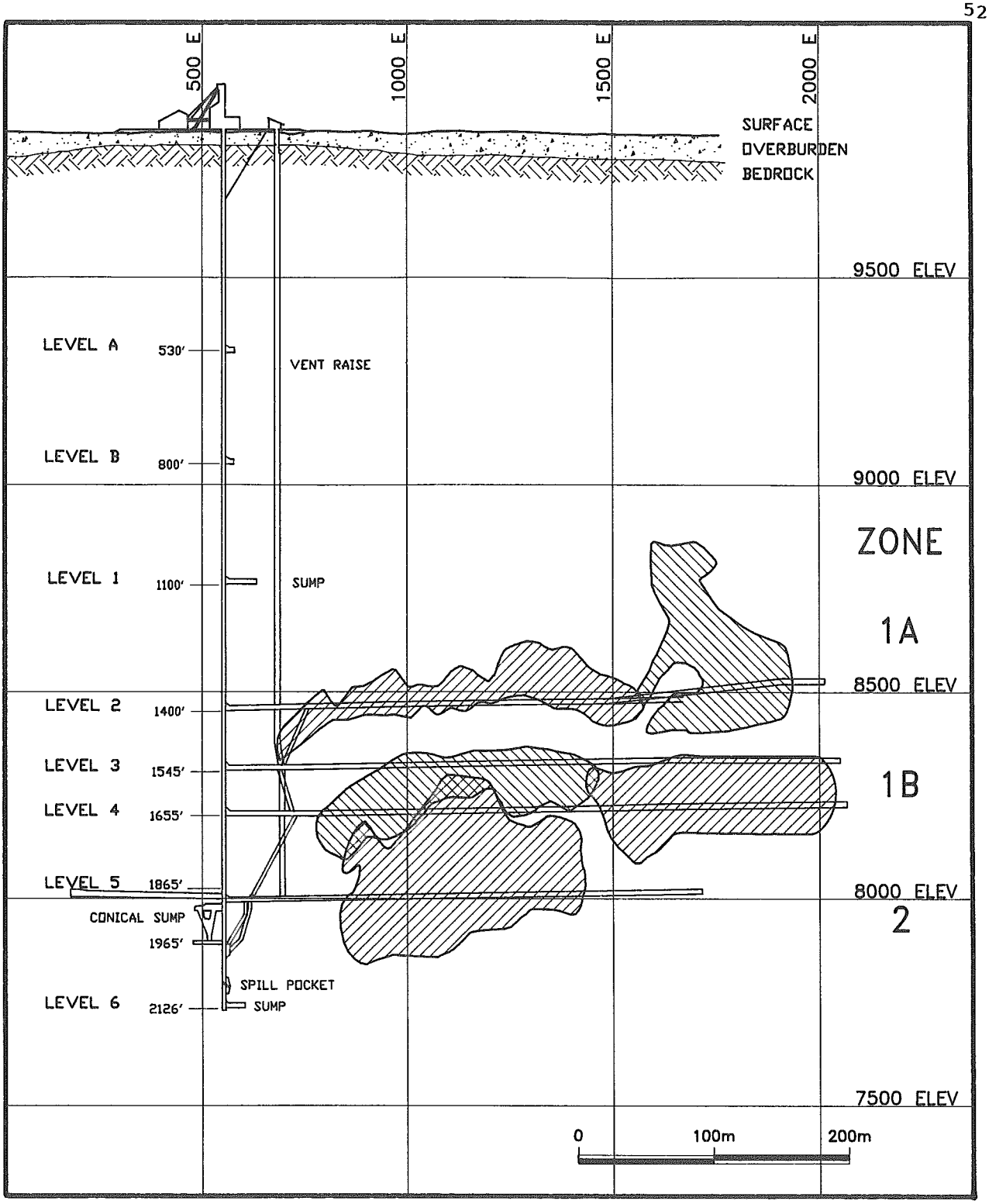

FIGURE 3 : Longitudinal projection looking NNE, Isle-Dieu mine.

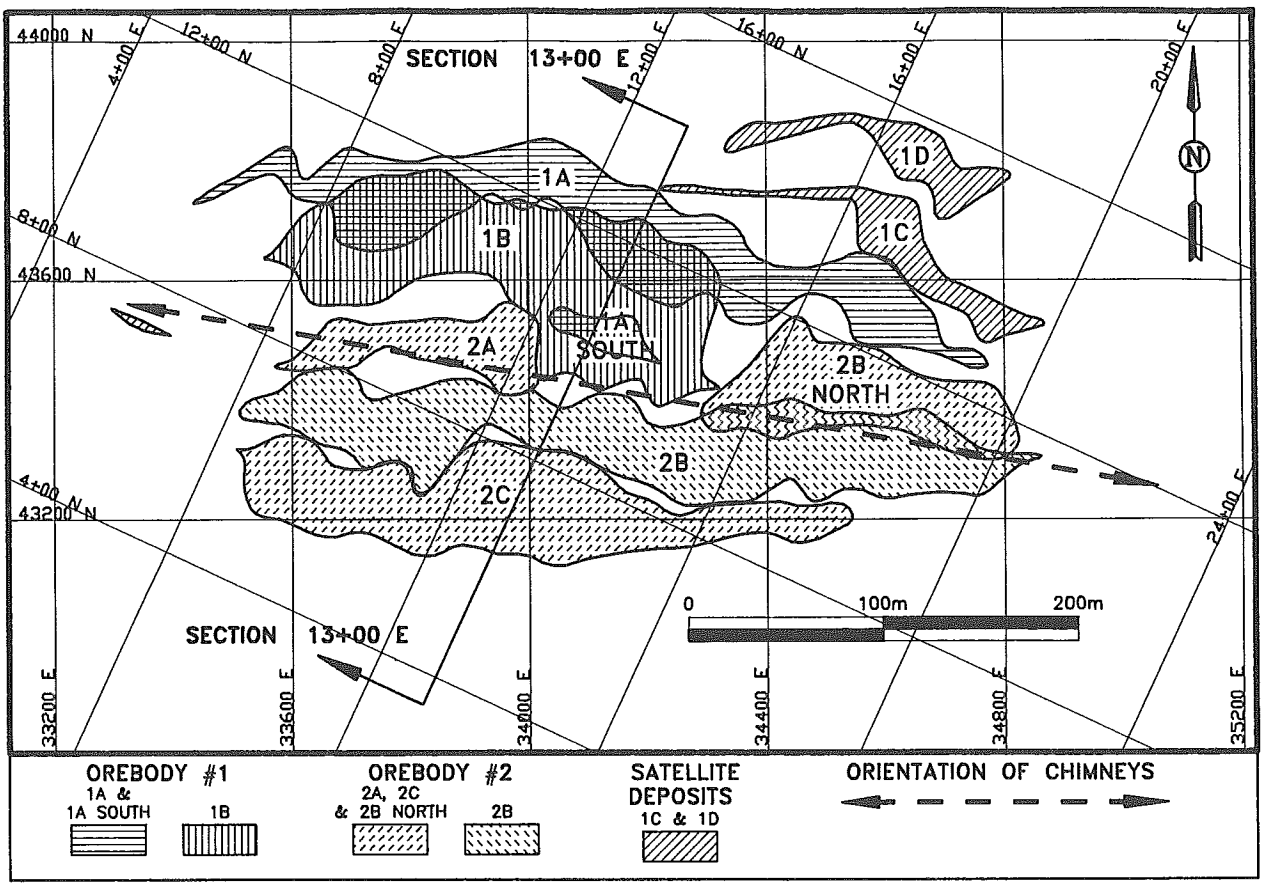

FIGURE 4 : Upper : Horizontal projection of the Isle-Dieu deposits.

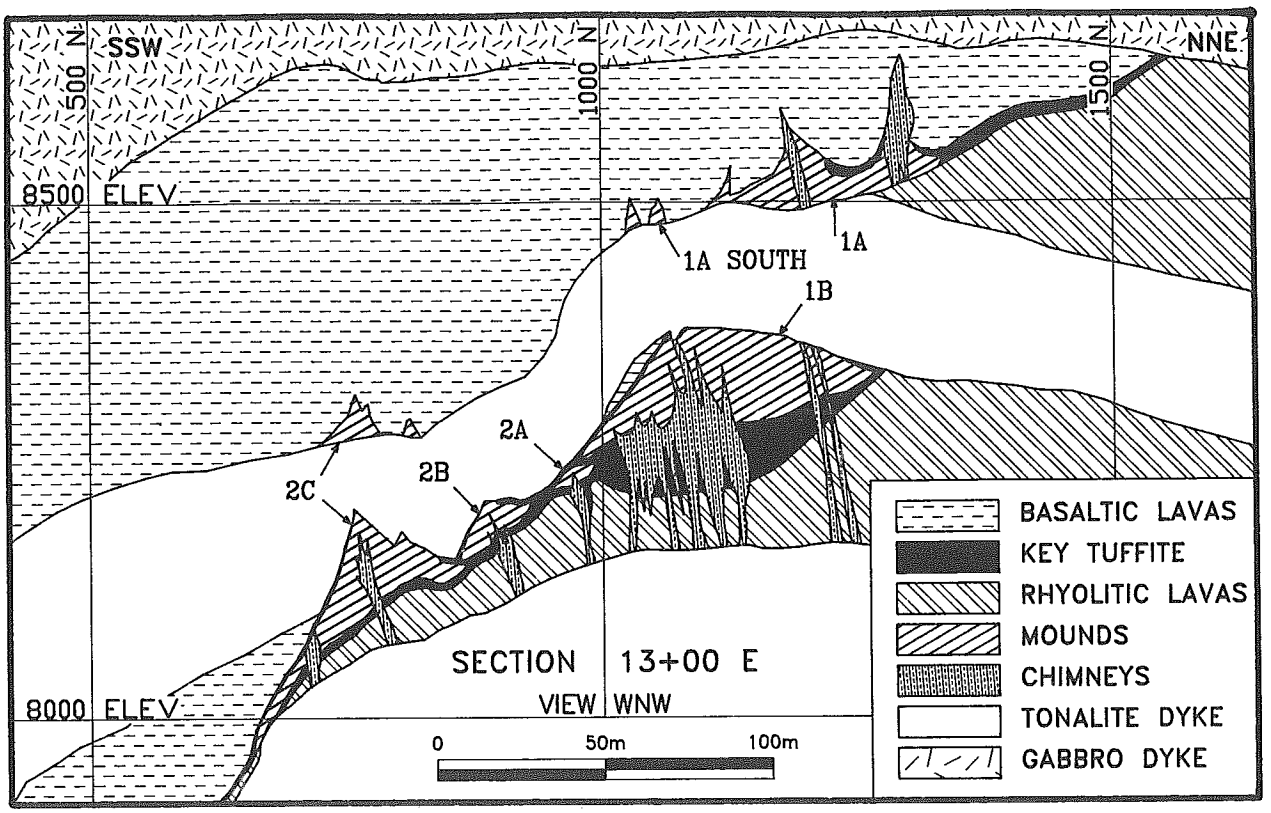

FIGURE 5 : Lower : Cross section 13+00E through Isle-Dieu deposits; redrawn from Lavallière et al., 1994.

chimneys are grouped in zones having a 20 to 40 m width and are divided in three types : sulphide chimneys, magnetite chimney and talc chimneys. Some chimneys cross-cut all of the lithological units, the rhyolite lavas at the base, the lower tuffite, the massive sulfides mounds, the upper tuffite and finally the basaltic lavas. On the other hand, some chimneys cut only a few units at the base of the volcanic pile. These chimneys trend WNW and they are parallel to the long axis of the sulphide lenses (Lavallière et al., 1992).

The entirety of the Isle-Dieu deposit is well preserved and has locally undergone a weak deformation. Three fault families are present. Two families are trending (N275°/85°) and (N295°/85°) with a maximum vertical displacement of 30 meters combined with a late dextral horizontal movement. Theses deformations are concentrated in the ore deposit alteration zones and cross-cut the stratigraphy of the whole deposit. The other fault family, not as frequent as the other two, trends (N315°/60°) and is locally in contact with felsic dykes containing erratic gold grades.

The Isle-Dieu ore deposit makes a remarkable exhibit in the mining camp because of its low deformation and associated hydrothermal alteration. Its morphological characteristics are representative of the entirety of the south flank's deposits (Lavallière & al., 1992). The spatial localization of the massive sulphide lenses is ruled by the superposition of both stratigraphic and structural controls. The stratigraphic control is noted by the exhalative horizon (Key Tuffite) which connects all the deposits. The structural control is shown by the presence of synvolcanic faults in the rhyolitic lavas to postvolcanic faults in the whole stratigraphy.

UNDERGROUND VISIT

The underground mine visit usually comprises a half hour audio-visual talk followed by a two hour underground tour. Even though some of the best exposures are not available anymore, the tour will tentatively cover the stratigraphic sequence in the orebody neighbourhood with an emphasis on the chimneys.

REFERENCES

Lavallière, G., Guha, J., Daigneault, R. et Bonenfant, A., 1994. Cheminées de sulfures massifs atypiques du gisement d'Isle-Dieu, Matagami, Quebec : Implications pour l'exploration. Exploration and Mining Geology, 3, No. 2, P. 109-129.

The 4CW massive sulphide showing in the paratochtonous belt of the Grenville Province

by

Sergio Cattalani

Cominco Ltd.

950 boul. Saguenay, C.P. 398, Rouyn-Noranda (Québec) Canada, J9X 5C4

Location and Access

The 4CW Cu-Zn-Pb showing is located in the Baudin Township (32B-4), and is part of Cominco Limited's Grenval project area, located immediately to the southeast of the Grenville Front (GF), within the parautochthonous domain of the Grenville Province (GP), approximately 120 km east of Val d'Or, Quebec (Fig. 1). The Forsythe outfitter camp is situated approximately 70 km east of Senneterre on the southern shore of Lake Attic.

Exploration Philosophy and Methodology

The general premise behind the exploration efforts at Grenval-Greneast and Grenorth is the suggestion that Archean rocks of the Superior Province's Abitibi Greenstone Belt (AGB) could extend across the GF, into the western GP, and as such may represent extensive and as yet largely unexplored tracts of land with high potential for hosting economic mineral deposits. The interpretation of an Archean to Proterozoic origin for rocks of the Parautochthonous Belt stems empirically from the existence of several Archean lithological complexes which can be traced across the GF (eg. the Doré Lake layered complex near Chibougamau, the Labrador Trough), and has been recently substantiated by reliable geochronological studies (e.g. Easton, 1986). In addition, recent Sm/Nd geochronological data (Birkett, T.C., unpublished data) as well as unpublished Pb/Pb data (interpreted by Ralph Thorpe, Geological Survey of Canada) for samples located within and proximal to the Grenval-Greneast project area clearly yield Archean ages (2340 and 2689 Ma, respectively) .

Recent regional mapping programs by the Geological Survey of Canada (GSC) and by the Ministère de l'Energie et des Ressources, Québec (MERQ; Birkett et al., 1991; Ciesielski, 1988; 1991; 1992; Ciesielski and Madore, 1989; Moorhead et al., 1991) has indicated the presence of significant amounts of amphibolitic and tonalitic gneiss of presumed volcanic origin. Moorehead et al., (1991), suggest that rocks of the Greneast project area may represent metamorphosed equivalents of rocks of the Archean aged, Tavernier-Tiblemont Belt. Furthermore, regional lithogeochemical surveys in this region by Laflèche and Birkett (in press) of the GSC report trace and rare earth element geochemistry, as well as Sm/Nd ratios that are consistent with Archean precursors for these rocks.

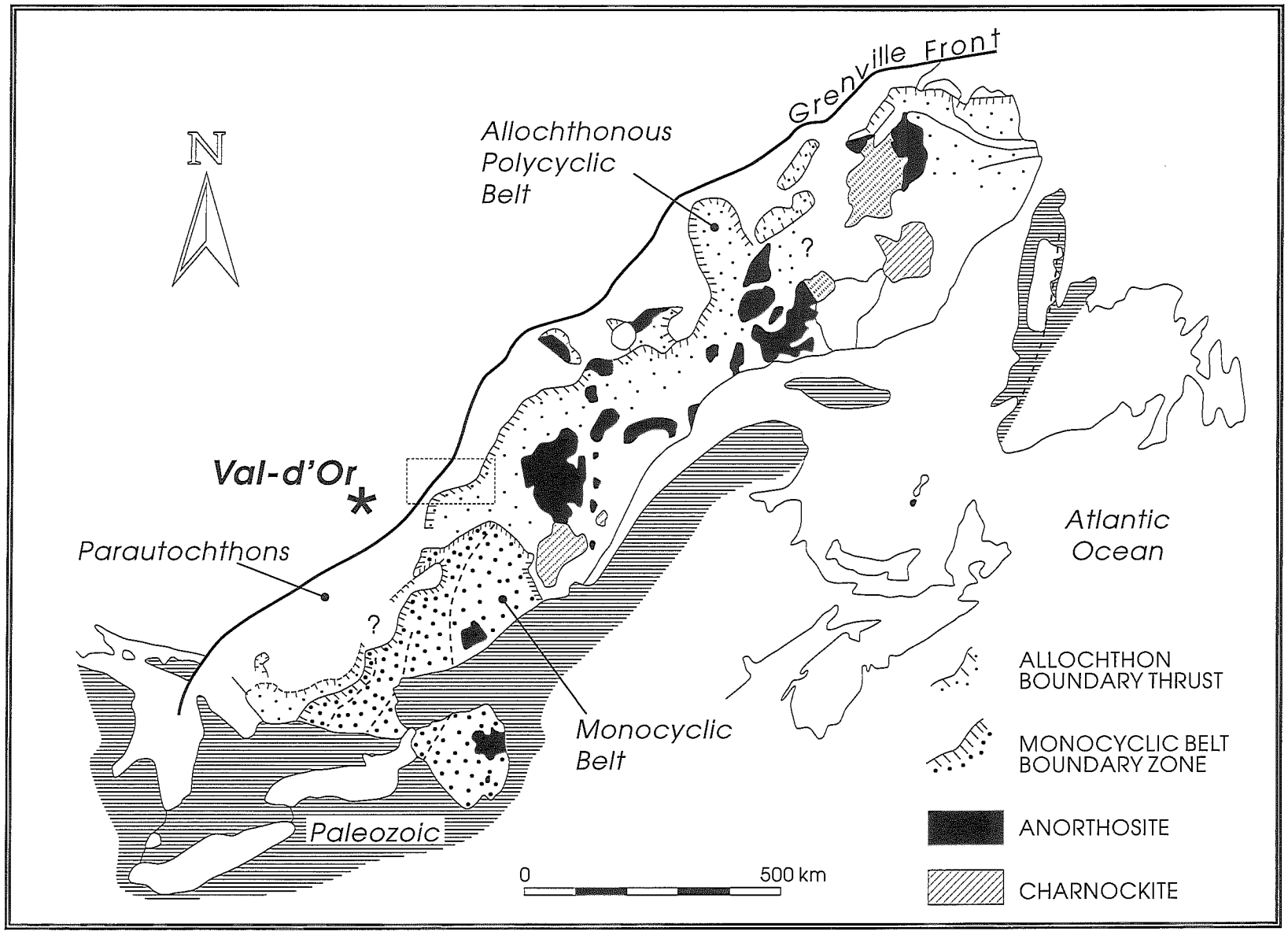

Figure 1. Location map of the Grenval project area, showing the locations of the parautochtonous and allochtonous domains of the Grenville Province. Reproduced from Birket and Camiré (1994).

The Grenval-Greneast-Grenorth projects represent the application of current, proven technology (irborne Electromagnetic) to the exploration for shallow burial base metal deposits in a new, virtually unexplored region. Individual airborne-electromagnetic anomalies were followed up by ground geophysics (Horizontal loop electromagnetic, magnetics, gravity), geochemistry, mapping and Beep-mat prospecting and eventually by drilling. In general, the area is covered by an extensive blanket of variable thickness of glaciofluvial sands and gravels. Although this type of overburden has proven problematical for soil geochemistry surveys, it provides ideal resistive conditions for geophysics.

Regional Geology

Recent work has divided the GP into three major belts, roughly distributed from north to south (Fig. 1; Rivers and Chown, 1986; Rivers et al., 1989): the Parautochthonous Belt, representing Archean and Proterozoic rocks that have been reworked during the Grenvillian orogeny; the Allochthonous Polycyclic Belt, representing upgraded and tectonized rocks of the foreland; and the Allochthonous Monocyclic Belt, represented by metavolcanic and metasedimentary rocks of the Wakeham and Grenville Supergroups (Fig. 1).

Rocks of the Parautochthonous domain have undergone an early phase of granulitization, followed by a prolonged period of amphibolitization (Marchildon, 1992). Metamorphic P-T conditions for which these rocks were subjected to have been estimated at 750 C and 8-10 kbars (Indares and Martignole, 1990; Marchildon, 1992). Rocks in the Greneast project area generally show low magnetic relief and are characterized by a relative abundance of amphibolitic gneiss. By contrast, rocks further to the south, consisting mainly of paragneiss, are visibly of higher metamorphic grade. The generally higher grade of these rocks allows for their distinction by way of a higher magnetic relief and a relative paucity of EM conductors.

The 4CW showing

The 4CW mineralized zone forms a significant base metal showing hosted by high-grade metavolcanic gneisses of felsic to intermediate composition forming a broad (~50m thick), complexly folded

stratabound structure plunging roughly to the southeast (Figs. 2 and 3). This zone, although showing good lateral continuity to the northwest, with a strike extent of approximately 1km, shows a sharp planar edge to the southwest defining an abrupt limit to the mineralization in that direction. Drilling intersections based on 1992 drilling (12 drill holes) indicate that the mineralized zone extends at least to a vertical depth of ~200m, averaging 0.7% Cu, 0.96% Zn and 220 ppb Au including intervals of 0.95m @ 5.5% Cu, 9.3% Zn; 1.0m @ 2.48% Cu, 13.0% Zn and 1.14m @ 1.7% Cu, 7.7% Zn. Drilling in early 1993 and 1994 has extended the mineralized zone to a vertical depth of ~500m and ~1000m, respectively. A summary assay table presenting detailed drilling results for the 4CW showing (ddh 1-15) is presented in Table 1. Selected composite vertical sections are also presented (Fig. 3).

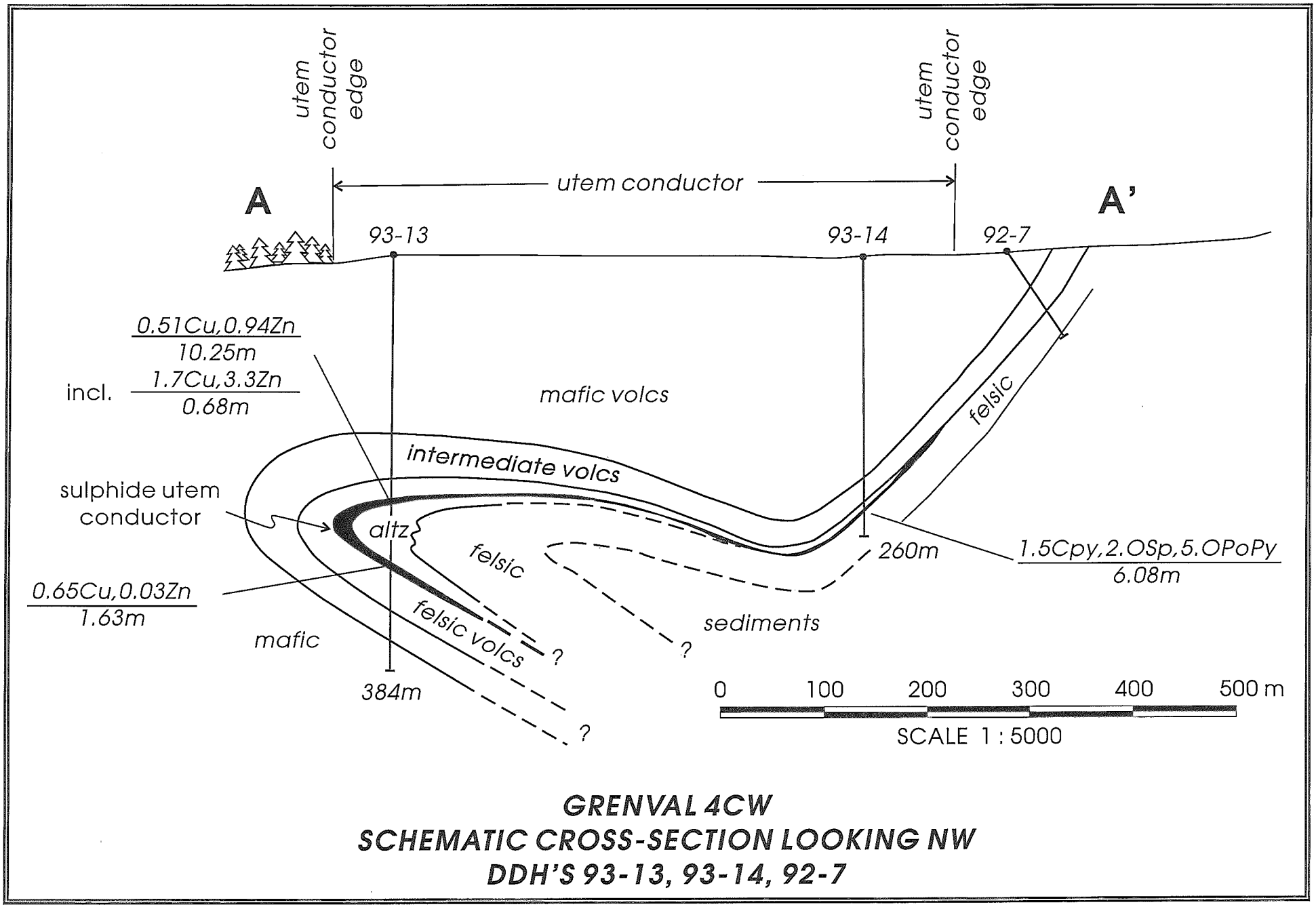

Figure 2. Idealized schematic, 1:5000 scale SSE-NNW cross-section of the 4CW mineralized structure showing the locations of drill holes 4CW92-7, 4CW93-13,14.

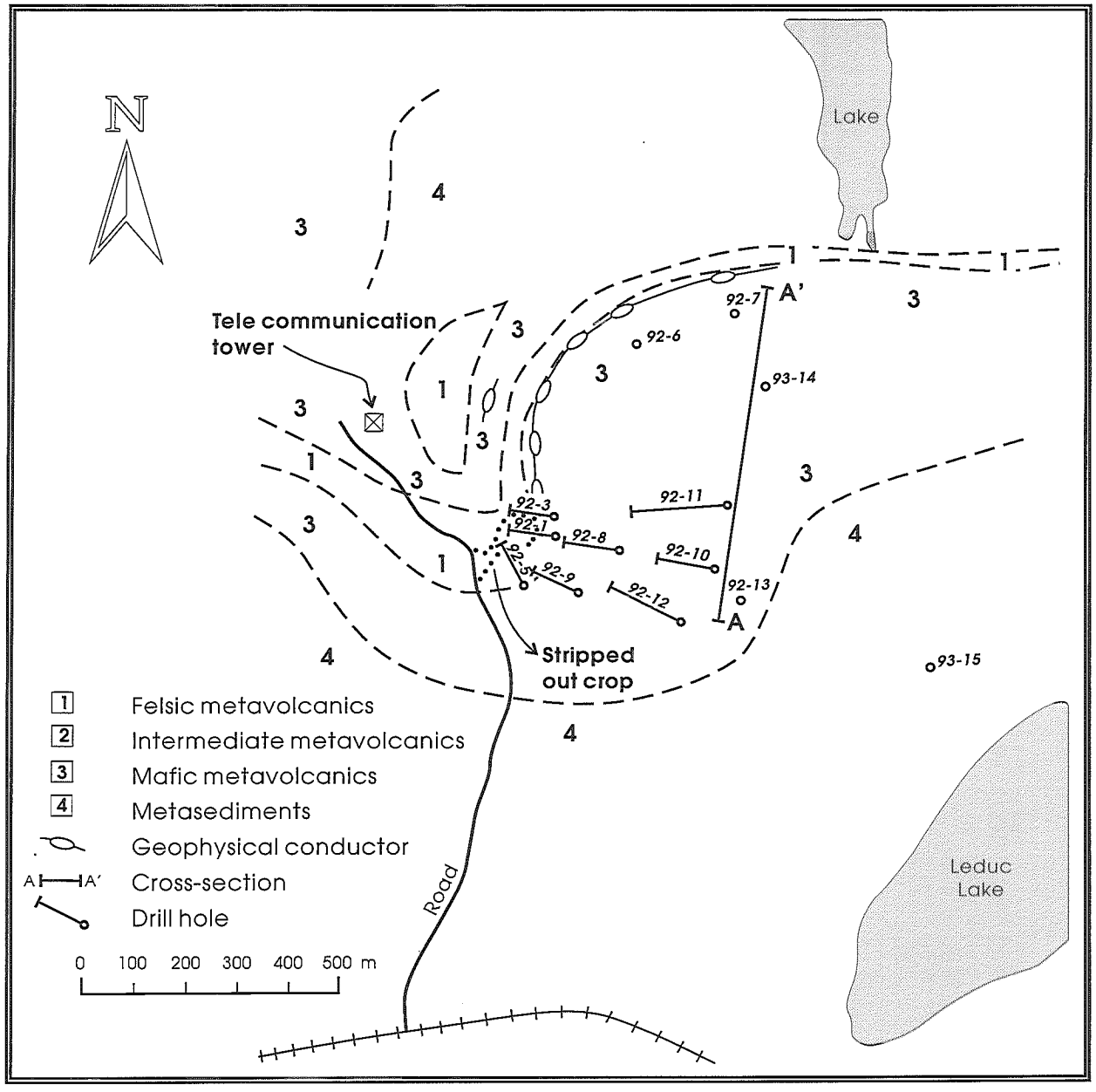

Figure 3. 1 : 500 scale plan map of the 4CW showing.

Table 1. Grenval 4CW Property - Assay Summary

Hole	Interval (m)	Length (m)	Cu ppm	Pb ppm	Zn ppm	Ag ppm	Au ppb
4CW-92-1	36.0-84.24	8.2	6970	750	9590	42	02
	incl. 36.8-43.1	6.3	14700	520	14780	60	9
	63.45-64.4	0.95	55000	620	93000	186	62
	70.7-71.7	1.0	24800	202	130000	88	9
4CW-92-2	37.45-56.1	18.65	1660	100	1755	9	8
	incl. 38.6-39.1	0.5	18400	120	755	100	791
	61.7-80.65	18.95	845	75	705	3	5
	85.6-93.65	8.05	840	85	1065	4	1
4CW-92-3	50.55-56.6	6.05	2010	350	4035	15	6
4CW-92-4	44.8-47.45	2.65	110	20	1230	<1	8
	71.6-73.7	2.1	260	65	1170	1	2
	79.3-80.45	1.15	2000	20	920	7	211
	112.4-113.1	0.7	358	85	9600	6	01<
4CW-92-5	51.8-91.0	39.2	3465	525	850	19	351
	incl. 66.89-67.05	0.16	117000	250	7000	360	151
	91.0-115.45	24.45	450	110	920	2	8
4CW-92-6	60.3-66.85	6.55	455	135	2250	5	3
4CW-92-7	no significant assay results						
4CW-92-8	84.85-132.68	47.83	4950	415	3930	18	9
	incl. 108.82-109.95	1.14	17000	164	77000	48	0
	114.95-127.95	13.0	8855	845	860	35	912
4CW-92-9	no significant assay results						
4CW-92-10	171.0-197.4	26.4	2170	175	3545	8	3
	incl. 171.0-187.65	16.65	2975	225	5375	12	7
	incl. 178.67-181.25	2.58	5524	403	16355	25	161
4CW-92-11	133.2-167.0	33.8	1170	135	3095	5	4
	incl. 133.2-143.6	10.4	1870	250	8900	13	5
4CW-92-12	138.2-151.26	13.06	1855	390	6570	10	3
	incl. 142.0-145.3	3.3	3081	409	15303	16	2
	179.42-220.47	41.14	1795	870	930	20	42
	incl. 182.4-188.14	5.74	2776	2263	755	64	
1118							
4CW-93-13	219.68-222.6	2.92	4198	702	16945	15	061
	225.98-228.31	2.33	9000	249	16120	21	6
4CW-93-14	223.0-225.84	2.83	1995	459	15503	24	6
4CW-93-15	493.98-501.44	7.46	1130	55	9839	8	3
	incl. 495.46-499.83	4.37	1301	71	12150	10	3

Geology and Rock Types

The 4CW showing is interpreted as being hosted by a complexely folded but laterally continuous package of felsic to intermediate gneisses of metavolcanic origin. Mafic gneisses form the hangingwall to the mineralized zone. Individual units are of decametric thickness and have kilometric strike extent. The

stratigraphy which hosts the 4CW mineralized zone forms a south-southwest facing, tightly folded structure to the west with the southern, upper limb forming an open, gently folded structure extending to the northeast. Felsic to intermediate metavolcanic units which host the mineralized zone thin considerably along strike to the northeast. In drill core, fine-grained metagabbroic dykes and quartz-feldspar pegmatites are observed locally.

Mafic gneisses are green and generally exhibit a medium to coarse-grained equigranular to garnet-porphyroblastic texture. This rock consists mainly of hornblende, plagioclase, garnet, clinopyroxene and biotite. The absence of quartz is characteristic to this rock type. Felsic (quartz-dominant) to intermediate (feldspar-dominant) gneisses are generally fine to medium-grained and equigranular to garnet porphyroblastic. They consist primarily of quartz, feldspar, garnet, biotite and/or phlogopite with local minor hornblende. Where proximal to mineralization, they may exhibit porphyroblasts of bone-white sillimanite, generally as fine needles or bundles, and locally as tabular aggregations pseudomorphous after kyanite porphyroblasts, as well as minor staurolite. Rocks closely associated with zones of mineralization commonly contain abundant garnet and phlogopite. Intensely altered rocks (ALTZ) are typically characterized by an assemblage of very coarse grained garnet, orthoamphibole (gedrite to cummingtonite), phlogopite and/or sillimanite with lesser, variable amounts of sulphides (pyrrhotite, chalcopyrite, sphalerite, pyrite and galena) ± gahnite ± hercynite ± staurolite ± kyanite ± cordierite ± magnetite ± corundum (observed in thin section only) ± minor dumortierite, identified in samples collected from the surface exposure (Birkett and Camiré, 1994). Dumortierite has been interpreted as evidence for substantial hydrothermal alteration in aluminosilicate-bearing volcanic rocks at Louvicourt, Quebec (Taner and Martin, 1993). The 4CW dumortierite (Birkett and Camiré, 1994) is chemically similar to that reported from high-grade cordierite-orthoamphibole gneisses in southern Norway (Visser and Senior, 1991). In drill core, two distinctive types of ALTZ have been identified. Type 1 consists primarily of biotite-orthoamphibole-garnet while type 2 consists of garnet-biotite-sillimanite with orthoamphibole minor to absent. The two distinctive ALTZ facies may reflect an original hydrothermal distribution of contrasting mineralogical assemblages, in turn relating to the intensity of alteration. Quartz is everywhere absent from the most intensely altered facies.

To the south of the surface exposure, and directly overlying the mafic gneiss, there occurs a thick (>150m) interval of paragneiss. This lithology consists of an assemblage of quartz-plagioclase-biotite-garnet with lesser alkali feldspar, sillimanite, carbonate and local minor graphite, pyrrhotite and pyrite. These rocks commonly display a tectonic banding on the centimetric to decimetric scale and locally rusty weathering.

Within the limits of, and proximal to the 4CW stripped outcrop, there occur good examples of mafic to felsic gneisses, paragneiss and the characteristic ALTZ facies. A map of the stripped outcrop showing the location of the various trenches is presented as Figure 4.

Structure

The rocks in the area of the 4CW property show evidence for at least two phases of intense deformation (Birkett and Camiré, 1994). Mineralization at 4CW is stratabound and mainly occupies the hinge of, and parts of the flanks of a south-southwest facing isoclinal, overturned, second-generation (F_2), antiformal fold structure which plunges moderately (~40°) to the east-southeast. The fold axial plane defined by the S_2 foliation is oriented at 302°/84°. The southern, or upright limb extends laterally to the northeast for at least 1km forming a moderately open, southeast plunging synform. An ENE-WSW third phase F_3 axial plane, parallel to the regional gneissic trend, overprints the 4CW structure. The thickest portion of the mineralized zone corresponds with the hinge zone of the F_2 fold structure. This suggests a structural history which included remobilization of the sulphides into the hinge zone, due to their lower relative viscosities. Alternatively, the thicker portion of the sulphides controlled the nucleation of the folds.

Lithogeochemistry and Alteration

The mineralized zone is intimately associated with a variable, yet distinctive assemblage of very coarse grained phlogopite-garnet ± orthoamphibole ± sillimanite ± sulphides ± gahnite ± hercynite ± staurolite ± kyanite ± cordierite ± magnetite ± corundum ± dumortierite. This latter facies is thought to represent the high-grade metamorphic equivalent of a chlorite-sericite alteration zone typically associated with VMS deposits of the AGB. At greater depth, this zone lacks the orthoamphibole and contains greater

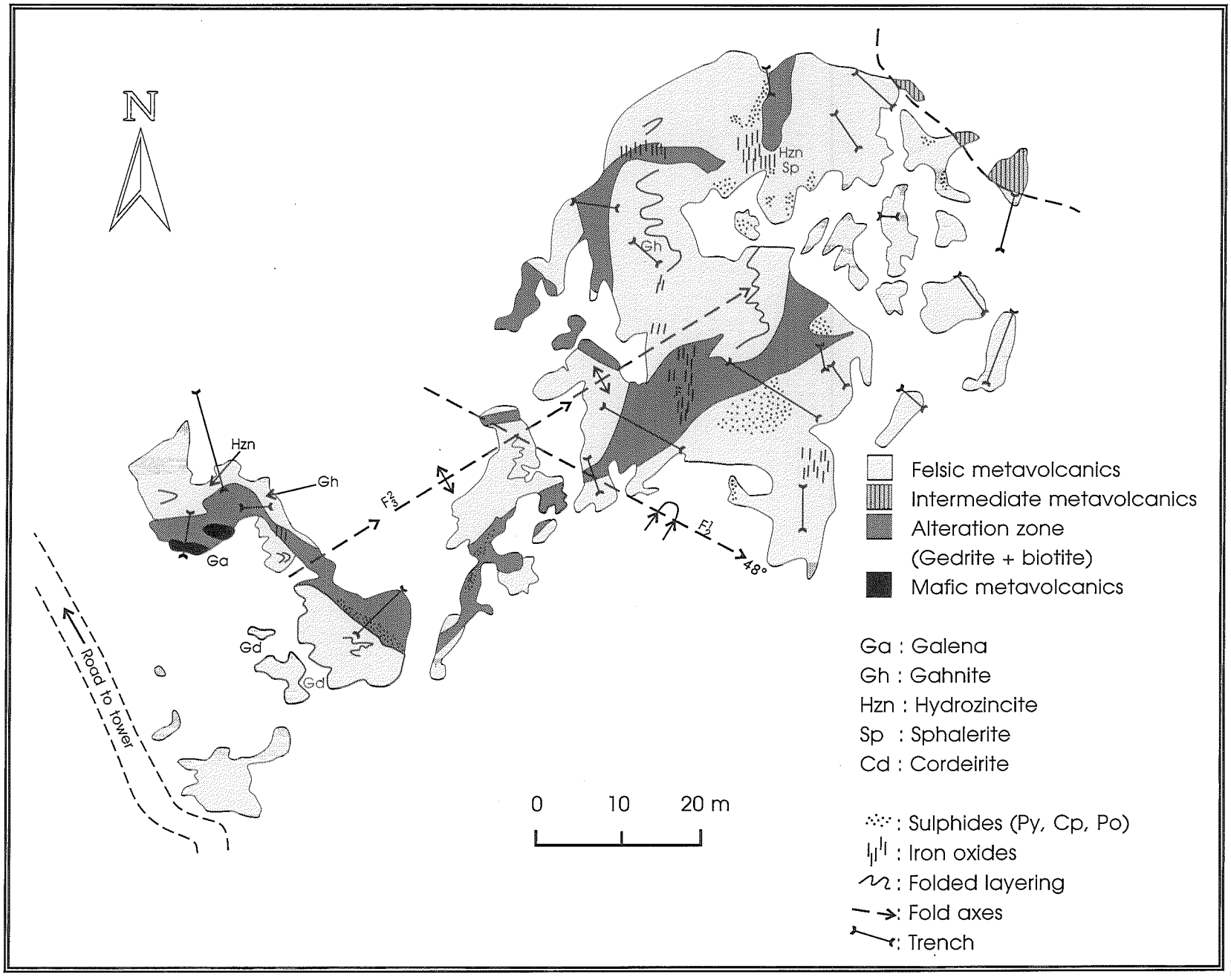

Figure 4. 1:500 scale plan map of the 4CW surface stripped zone, showing the locations and characteristics of the various surface trenches.

absolute contents of aluminosilicate minerals (sillimanite-kyanite) and of staurolite.

Previous interpretation of geochemical data from rocks at 4CW (Moore, 1992; Cattalani and Moore, 1993), has indicated distinct compositional clusters for mafic, intermediate and felsic gneisses, and has suggested a single, continuous magmatic series for these rocks. Furthermore, mineralized (MINZ) and altered (ALTZ) zone samples have been shown to correspond to intermediate to felsic precursor compositions, which appear to have undergone considerable leaching of silica and Na, and strong apparent enrichments in Fe and Mg, typical of hydrothermal alteration associated with VMS processes. Recently collected samples confirm the compositional spectrum previously established for 4CW host rocks, as illustrated on Na_2O+K_2O vs SiO_2 and SiO_2 vs. log Zr/TiO2 diagrams (Figs. 5 and 6, respectively). Furthermore, the distribution of ALTZ samples on Al vs. Si and Si vs. Fe+Mg+Mn cation alteration diagrams (Figs. 7 and 8, respectively) suggests that the observed orthoamphibole-garnet and sillimanite-garnet assemblages (ALTZ) are consistent with having formed by metamorphism of a chlorite-rich alteration assemblage. Interestingly, no distinct spatial zonation in the intensity of alteration is evident from the data (ie. near-surface samples do not appear to be more or less altered than samples originating deeper downplunge). In fact, there is no clear, documentable decrease in this parameter even to ~1 km downplunge (4CW-93-15) from the surface showing.

Results of mass change calculations (cf. MacLean, 1990), for a total of 20 samples of ALTZ indicate that this lithotype has lost mass reflected by a residual concentration of immobile elements. Hydrothermally altered rocks associated with VMS deposits in Archean greenschist teranes which show similar characteristics and degrees of mass loss are invariably chloritized and/or sericitized and generally depleted in silica (MacLean and Kranidiotis, 1987; Barrett and MacLean, 1991). The calculations were based on components TiO_2 and Zr, which have been shown to be essentially immobile in greenschist grade hydrothermally altered rocks for a number of Archean VMS deposits (Barrett et al., 1991a,b,c; 1992; 1993a,b; MacLean and Hoy, 1991; MacLean and Kranidiotis, 1987), as well as for high-grade metamorphic polymetallic deposits such as Montauban (Bernier and MacLean, 1993), and Dussault (Bernier, 1992) in the GP of Quebec. Overall, average mass changes for all samples collectively, as well as separately for samples with intermediate or felsic precursors show substantial losses in silica, strong gains in FeO and

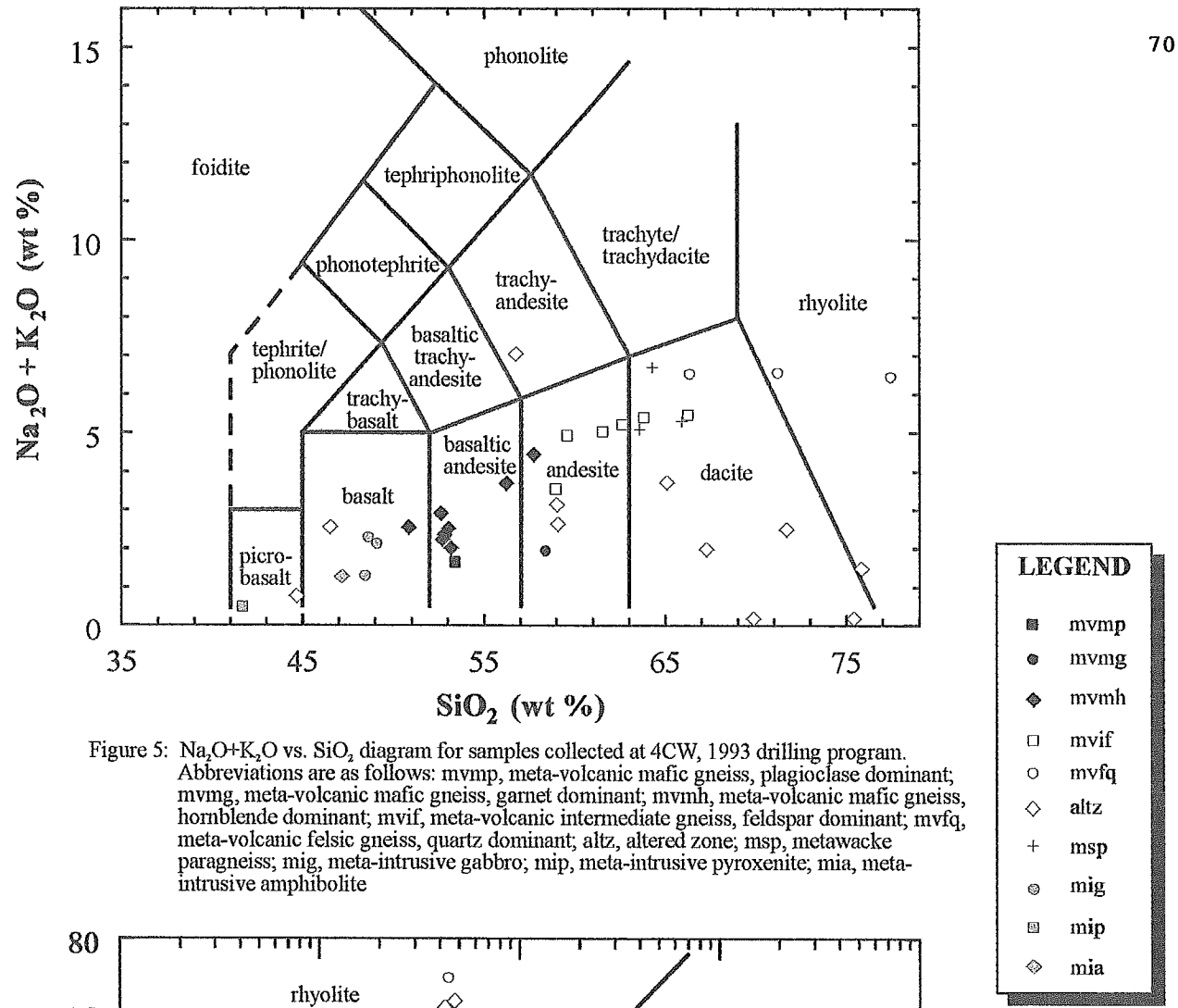

Figure 5: Na_2O+K_2O vs. SiO_2 diagram for samples collected at 4CW, 1993 drilling program. Abbreviations are as follows: mvmp, meta-volcanic mafic gneiss, plagioclase dominant; mvmg, meta-volcanic mafic gneiss, garnet dominant; mvmh, meta-volcanic mafic gneiss, hornblende dominant; mvif, meta-volcanic intermediate gneiss, feldspar dominant; mvfq, meta-volcanic felsic gneiss, quartz dominant; altz, altered zone; msp, metawacke paragneiss; mig, meta-intrusive gabbro; mip, meta-intrusive pyroxenite; mia, meta-intrusive amphibolite

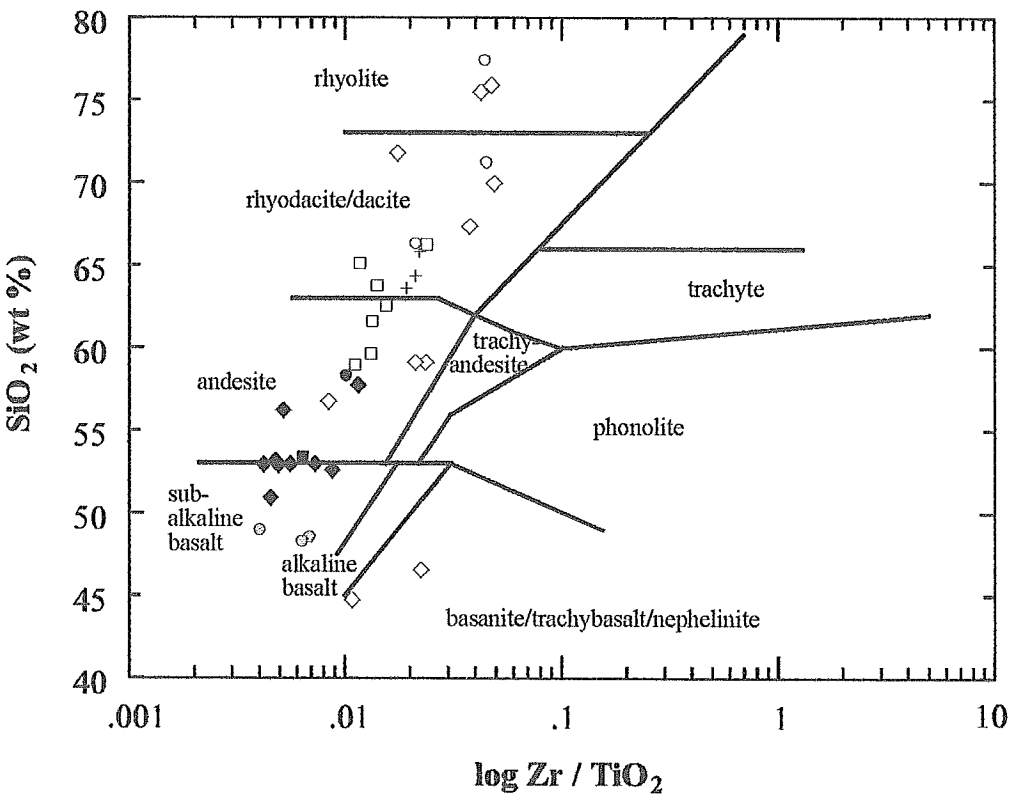

Figure 6: SiO_2 vs. log Zr/TiO_2 diagram for samples collected at 4CW, 1993 drilling program. Symbols as described for Figure 5.

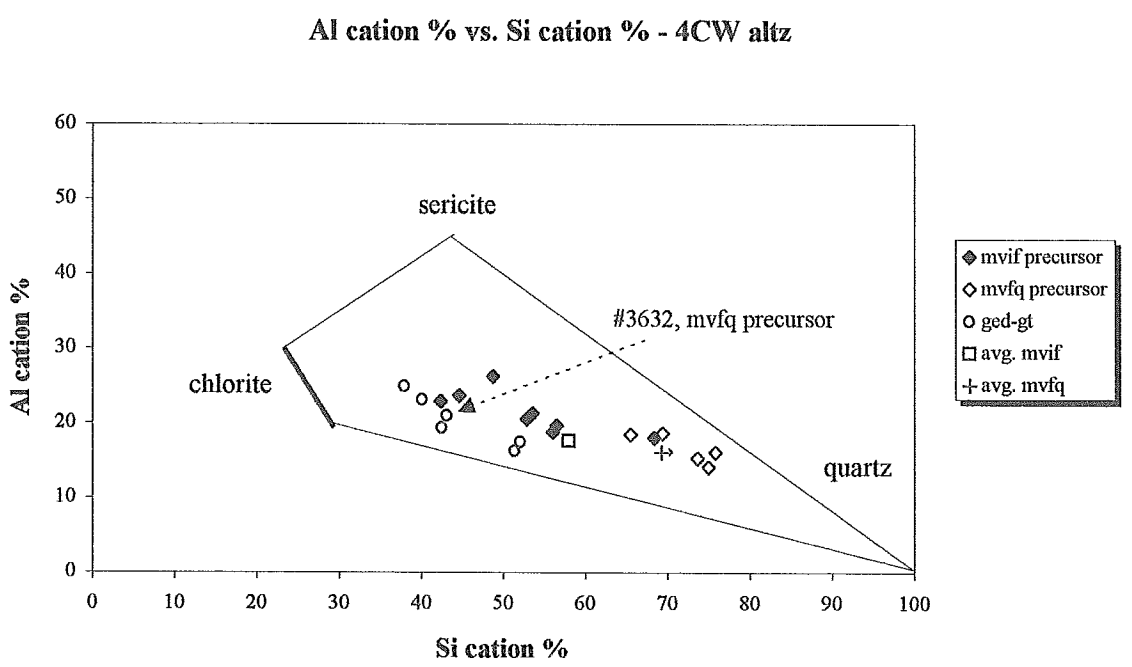

Figure 7. Al cation percent versus Si cation percent binary diagram for samples of altered zone gneisses, 4CW. Larger squares and crosses indicate average precursor compositions for meta-volcanic intermediate (mvif) and felsic gneisses (mvfq), respectively. Closed and open diamonds indicate the composition of the precursors for individual samples of for mvif and mvfq, respectively. Circles indicate samples of orthoamphibole-garnet-bearing altered zone gneises (altz). Sample 3632 is the only sample of of altz containing orthoamphibole which has a felsic (mvfq) precursor.

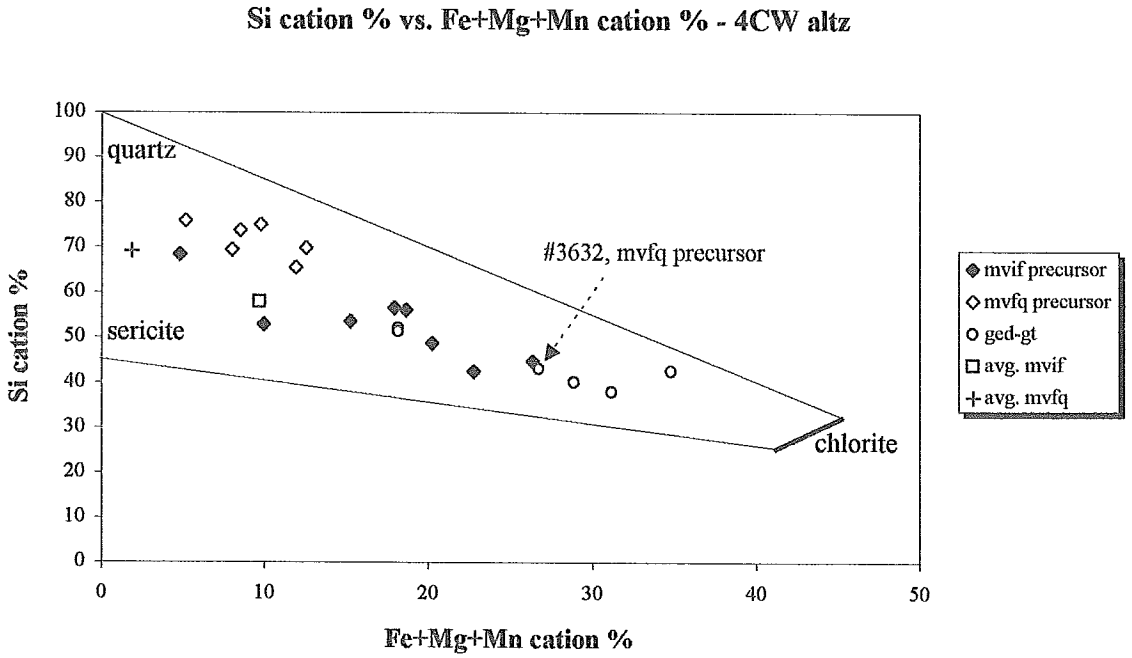

Figure 8: Si cation percent versus Fe+Mg+Mn cation percent binary diagram for samples of altered zone gneisses, 4CW. Symbols as described for figure 7.

MgO (sulphide addition and chloritization), and significant to moderate losses in alkalis (Table 2). Generally, samples corresponding to intermediate precursor compositions appear to have undergone a greater degree of mass loss than samples corresponding to felsic precursor. These chemical changes correlate well with that depicted by figures 7 and 8 and therefore strongly substantiate VMS-type hydrothermal alteration for host rocks at 4CW.

Table 2. Grenval 4CW Property - Mass Change Summary

component	average mass changes			average precursor	
	all samples	mvif	mvfq	mvif	mvfq
SiO2 (%)	-11.96	-20.90	-8.37	61.57	74.13
TiO2	0.00	0.00	0.00	0.76	0.27
Al2O3	0.29	-0.58	-0.72	15.92	14.60
FeO	5.76	3.55	7.88	7.49	1.46
MnO	0.17	-0.01	0.31	0.19	0.04
MgO	4.74	3.36	5.70	3.00	0.56
CaO	-1.90	-3.57	0.04	6.55	2.61
Na2O	-3.10	-1.69	-4.71	3.49	4.28
K2O	-0.34	-0.06	-0.94	0.88	1.94
P2O5	0.02	0.04	-0.03	0.14	0.09
Ba (ppm)	-294	-198	-414	261	732
Sr	-330	-179	-500	392	404

Mass changes, being quantitative rather than qualitative, can also be used to evaluate changes in the intensity of alteration in a given direction. At 4CW, the conductive, mineralized sheet dips at a moderate angle toward the ESE, extending for at least 1 km in that direction. In order to evaluate the mass changes that occured during alteration, samples of ALTZ are located onto an E-W vertical section passing through BL0 and L4+00E (collar of ddh 4CW-93-4), together with their distance from that surface reference point. This vertical section is subparallel to the true dip of the altered/mineralized structure and hence is optimally oriented to represent any downplunge zonation in the character or intensity of alteration. Figure 9 presents absolute mass changes for a) SiO_2 and FeO+MgO, b) Na_2O and K_2O and c) Sr and Ba for samples of ALTZ plotted as a function of distance from a reference point at surface. Apart from strong positive values in SiO_2, Na_2O, K_2O, Sr and Ba at 540 m (corresponding to ddh 4CW-93-14), the data shows little variation in the intensity of mass changes from surface (0 m) down to ddh 4CW-93-15 (870 m); this is again in accord with the distribution of data as seen on figures 7 and 8.

The generally sustained intensity of alteration for a distance of nearly 1 km downplunge from surface may reflect a structural attenuation or transposition of the hydrothermal alteration zone associated with the 4CW mineralizing system, particularly in the downplunge direction. Alternatively, this may suggest that the alteration zone was originally very extensive and widespread along strike, and hence possibly stratabound in nature. In this respect, the alteration zone at 4CW may have been distinctly different from the typical, Noranda-type, high-angle, focussed alteration pipes and may have resembled more alteration zones such as at Mattabi (Franklin et al., 1975) or Mattagami Lake (Roberts and Reardon, 1978; Costa et al., 1983).

Mineralization

The 4CW mineralized zone is a significant, high metamorphic grade base metal showing. Mineralization occurs over a broad zone (~50m thick), hosted by metavolcanic gneiss of felsic to intermediate composition. Drilling intersections indicate that the 4CW mineralized zone extends at least to a vertical depth of ~1000m. Sulphides include pyrrhotite, pyrite, chalcopyrite, sphalerite and minor galena, and exhibit coarse-grained disseminated to net-textured (recrystallized Durchbewegung texture)

a) SiO_2, FeO+MgO mass changes - EW section through 4CW

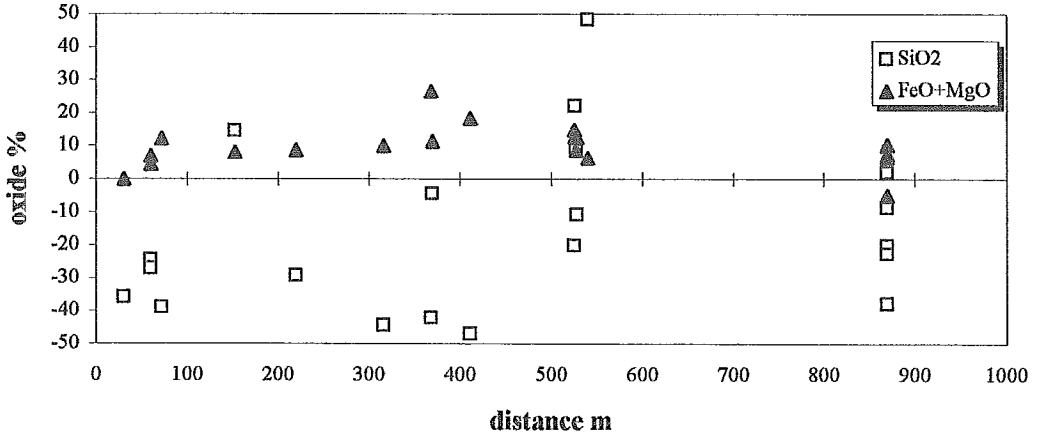

b) Na_2O, K_2O mass changes - E-W section through 4CW

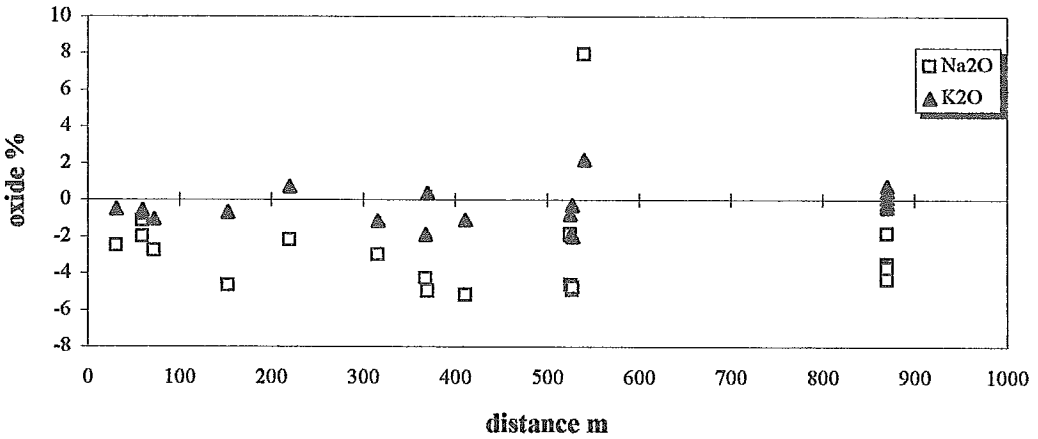

c) Sr, Ba mass changes - E-W section through 4CW

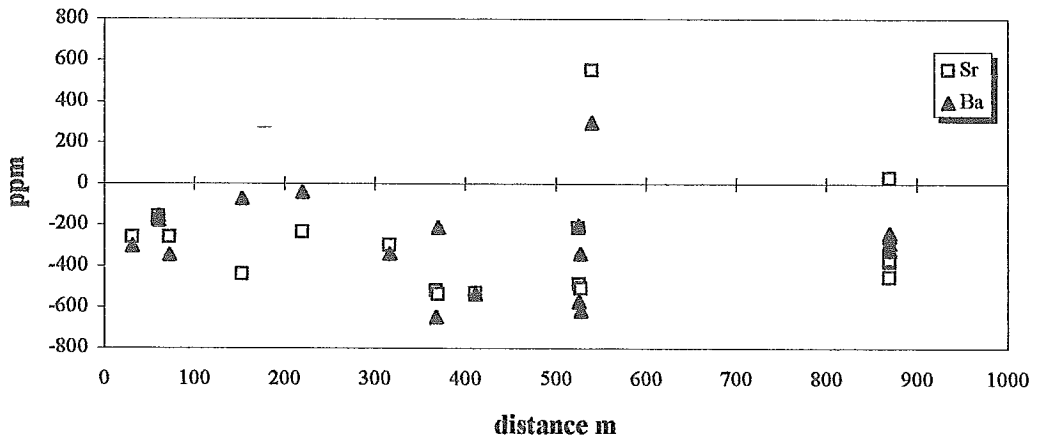

Figure 9. Absolute mass changes as oxide percent or ppm versus distance along an E-W vertical section, subparallel to the true dip direction of the 4CW folded, mineralized structure for a) SiO2 and FeO+MgO, b) Na_2O and K_2O, c) Sr and Ba.

to stringer textures over decimetric to plurimetric intervals. Significant amounts of silicate Zn also occurs as gahnite. The best mineralized intersections include 0.95m @ 5.5% Cu, 9.3% Zn; 1.0m @ 2.48% Cu, 13.0% Zn, 1.14m @ 1.7% Cu, 7.7% Zn and 0.62m @ 1.7% Cu and 3.3% Zn (Table 2).

Metal ratios, host unit isopachs and grade x thickness values for the 4CW mineralized zone clearly show the presence of a southeast-plunging mineralized zone. This trend also corresponds to the greatest thickness of the principal host unit and mineralized zone rocks. Grade x thickness values indicate that the highest concentrations of Cu are located in hole 4CW-92-1, with decreasing Cu:Zn ratios down-plunge and laterally to the east. The best Au and Ag values are also coincident with this southeast-trending hinge zone. Furthermore, the greatest thickness of intensely altered rock (ALTZ), interpreted as a high-grade metamorphosed equivalent to a footwall chloritic-sericitic alteration zone, is also coincident with this trend.

All holes which intersect mineralization, except 4CW-92-5, show a normal, vertical metal zonation (ie. Zn-rich top and Cu-rich base). Locally, chalcopyrite-rich stringer mineralization can be recognized as occurring below a thin massive sulphide interval (eg. hole 4CW-92-8). Inverted metal ratios recorded by hole 4CW-92-5 suggest that it intersects the inverted limb of the main fold, just below and east of the southeast-plunging fold hinge. Hole 4CW-92-12 shows an upper Zn-rich zone, followed by an underlying Cu-rich zone, followed again by a second, separate Zn-rich zone. Finally, drill hole 4CW-93-13 intersects a sequence consisting of an upper sulphide conductor, underlain by a thick interval of ALTZ, followed by a second sulphide conductor. This sequence is somewhat symmetric about a flat-lying plane corresponding to the axis of the overturned recumbent fold structure.

In summary, the character and geometry of the metal zonation observed for the 4CW mineralized zone, and of the associated alteration facies suggest a proximal Cu-Zn volcanogenic massive sulphide occurrence which has undergone significant deformation and transposition in the direction of the plunge trend. Although the near-surface, downplunge metal distribution suggests that the most Cu-rich part of the surface showing may have been eroded off, the effect of significant deformation and transposition of the mineralized trend in the downplunge direction, and hence the possibility of additional "proximal" sulphide zones at depth cannot be underestimated.

References

Barrett, T.J. and MacLean, W.H. 1991. Chemical, mass, and oxygen-isotopic changes during extreme hydrothermal alteration of an Archean rhyolite, Noranda. *Economic Geology*, **86**: 406-414.

Barrett, T.J., MacLean, W.H., Cattalani, S. and Hoy, L. 1993a. Massive sulfide deposits of the Noranda area, Québec. V. The Corbet Mine. *Canadian Journal of Earth Sciences*, **30**, 1934-1954.

Barrett, T.J., Cattalani, S. and MacLean, W.H. 1993b. Lithogeochemistry and alteration at the Delbridge massive sulfide deposit, Noranda, Quebec. *Journal of Geochemical Exploration*, **48**, 135-173.

Barrett, T.J., Cattalani, S., Hoy, L.H., Riopel, J. and Lafleur, P.-J. 1992. Massive sulfide deposits of the Noranda area, Québec. IV. The Mobrun Mine. *Canadian Journal of Earth Sciences*, **29**: 1349-1374.

Barrett, T.J., Cattalani, S. and MacLean, W.H. 1991a. Massive sulfide deposits of the Noranda area, Quebec. I. The Horne Mine. *Canadian Journal of Earth Sciences*, **28**: 465-488.

Barrett, T.J, Cattalani, S., Chartrand, F. and Jones, P. 1991b. Massive sulfide deposits of the Noranda area, Québec. II. The Aldermac Mine. *Canadian Journal of Earth Sciences*, **28**: 1301-1327.

Barrett, T.J, MacLean, W.H., Cattalani, S., Hoy, L.H. and Riverin, G. 1991c. Massive sulfide deposits of the Noranda area, Québec. III. The Ansil Mine. *Canadian Journal of Earth Sciences*, **28**: 1699-1730.

Bernier, L.R. 1992. Caractéristiques géologiques, lithogéochimiques et pétrologiques des gîtes polymétalliques de Montauban et de Dussault. Séminaire d'information 1992, résumé des

conférences. *Ministère de l'Énergie et des Ressources, Québec*, **DV 92-03**, 31-34.

Bernier, L.R. and MacLean, W.H. 1993. Lithogeochemistry of a metamorphosed VMS alteration zone at Montauban, Grenville Province, Quebec. *Exploration and Mining Geology*, **2**, No. 4, 367-386.

Birkett, T.C., Marchildon, N., Paradis, S. and Godue, R. 1991. The Grenville Province to the east of Val d'Or, Québec: A geological reconnaisance and a possible extension of the Abitibi greenstone belt in the Grenville parautochthonous belt. *Geological Survey of Canada, Current Research*, **91-1C**, 1-7.

Birkett, T.C. and Camiré, G.E. 1994. The Cominco 4CW prospect: a report on mineralogy, geochemistry and structural geology. Internal report,

Cattalani, S. and Moore, D.W. 1993. Grenval Project, 1992 Drilling Report. Cominco Ltd., Eastern District, internal report.

Ciesielski, A. 1988. Geological and structural context of the Grenville Front, southeast of Chibougamau, Quebec. **Geological Survey of Canada**, *Paper 88-1C*, 353-366.

Ciesielski, A. 1991. The Grenville Front and the extension of the rocks of the Superior Province in the NW Grenville Province: The case of Chibougamau and Val d'Or areas, Quebec. In Proceedings of the Abitibi-Grenville-Lithoprobe Workshop, Montreal, October 1990, p. 43-48.

Ciesielski, A. and Madore, C. 1989. Litho-tectonic map of the Grenville Front, the Archean parautochthonous orthogneisses and Proterozoic dykes in the Central Grenville Province, southeast of Chibougamau, Quebec. *Geological Survey of Canada*, **Open File Map 2059**.

Cieiselski, A. 1992. Tonalitic orthogneiss in the Central Grenville Province: A reworked Archean substrate to the Abitibi Greenstone Belt, eastern Superior Province, Quebec. Geology Dept. (Key Centre) & University Extension, The University of Western Australia, Publ. 22, 161-176.

Costa, U.R. Barnett, R.L. and Kerrich, R. 1983. The Mattagami Lake mine Archean Zn-Cu sulfide deposit, Quebec: Hydrothermal coprecipitation of talc and sulfides in a sea-floor brine pool-Evidence from geochemistry; 18O/16O, and mineral chemistry. *Economic Geology*, **78**, 1144-1203.

Easton, R.M. 1986. Geochronology of the Grenville Province. In Moore, J.M., Davidson, A. and Baer, A.J. (eds.), The Grenville Province. *The Geological Association of Canada*, **Spec. Paper 31**, 127-173.

Franklin, J.M., Kasarda, J. and Poulsen, K.H. 1975. Petrology and chemistry of the alteration zone of the Mattabi massive sulphide deposit. *Economic Geology*, **70**, 63-79.

Indares, A. and Martignole, J. 1990. Metamorphic constraints on the evolution of gneisses from the parautochthonous and allochthonous polycyclic belts, Grenville Province, western Quebec. *Canadian Journal of Earth Sciences*, **27**, 357-370.

Lafleche, M.R. and Birkett, T.C. Geochemistry and petrogenesis of Archean and Proterozoic mafic to ultramafic granulites and amphibolites south of the Grenville Tectonic Front, Quebec. In press.

Marchildon, N. 1992. A study of mineral zoning and metamorphism in the Grenville Front area, east of Senneterre, Québec. Unpub. M.Sc. thesis, Rensellaer Polytechnic Institute, Troy, New York, 132 pp.

MacLean, W.H. 1990. Mass change calculations in altered rock series. *Mineralium Deposita*, **25**, 44-49.

MacLean, W.H. and Hoy, L.H. 1991. Geochemistry of hydrothermally altered rocks at the Horne mine, Noranda, Québec. *Economic Geology*, **86**, 506-528.

MacLean, W.H. and Kranidiotis, P. 1987. Immobile elements as monitors of mass transfer in hydrothermal alteration: Phelps Dodge massive sulfide deposit, Matagami, Quebec. *Economic Geology*, **82**, 951-962.

Moore, D.W. 1992. Grenval Project, 1991 Summary Report, Cominco Ltd. Eastern District, internal report.

Moorehead, J., Girard, R. and Birkett, T.C. 1991. Prolongement vers l'est des ceintures de roches vertes de l'Abitibi à l'interieur de la Province de Grenville: Nouvelles cibles d'exploration à l'est de Senneterre. *Ministère de l'Energie et des Ressources, Québec*, **PRO 91-17**, 4 pp.

Roberts, R.G. and Reardon, E.J. 1978. Alteration and ore-forming processes at Mattagami Lake mine, Quebec. *Canadian Journal of Earth Sciences*, **15**, 1-21.

Taner, M.F. and Martin, R.F. 1993. Significance of dumortierite in an aluminosilicate-rich alteration zone, Louvicourt, Quebec. *Canadian Mineralogist*, **31**, 137-146.

Visser, D. and Senior, A. 1991. Mg-rich dumortierite cordierite-orthoamphibole-bearing rocks from the high-grade Bamble Sector, south Norway. *Mineralogical Magazine*, **55**, 563-577.

The Grevet Zn - Cu massive sulfide deposit

Lacroix, J. and Daigneault, R.

CERM/Université du Québec à Chicoutimi, 555 boul. de l'Université, Chicoutimi, Qc, Canada G7H 2B1

Introduction

The Grevet Zn-Cu massive sulfide deposit is located 40 km northwest of the town of Lebel-sur-Quévillon, in the central portion of the Abitibi greenstone belt. It was discovered in 1989 by Serem Québec Inc. and VSM Exploration Inc, and has total geological reserves of 18 475 400 million tonnes grading 7.22% Zn, 0.41% Cu, 31.3 g/t Ag and 0.15% Pb. The sulphide lenses are included in highly strained and transposed host rocks within the Cameron fault zone, a regional southeast trending ductile deformation zone (Daigneault and Archambault 1990, Chown et al. 1992, Lacroix et al. 1993). The following overview results mostly from surface investigations undertaken by J. Lacroix for his Master's degree at the University du Québec à Chicoutimi. For more details, the reader is referred to Lacroix et al. (1993).

Regional geology

The supracrustal assemblages which hosted the Grevet Mines are dominated by mafic to felsic volcanic rocks, gabbroic and dioritic intrusive rocks. Rocks are metamorphosed to greenschist facies except near the Mountain pluton, an elongate tonalitic body situated several hundred meters to the south, where an amphibolite contact metamorphic aureole occurs.

Cameron deformation zone (CDZ)

The Cameron deformation zone (CDZ) is one of several major structural discontinuities occurring in the Abitibi Subprovince (Daigneault and Archambault, 1990). Oriented in a southeasterly direction, the CDZ is over 80 km long and locally up to 5 km thick. Rocks in the CDZ are distinguished from surrounding rocks by their SE-trend and their intensely deformed nature characterized by near complete obliteration of primary features. On the Grevet area (Fig. 1), the CDZ is characterized by mylonitic, subvertical foliation planes striking at N118°, which contains subhorizontal stretching lineations.

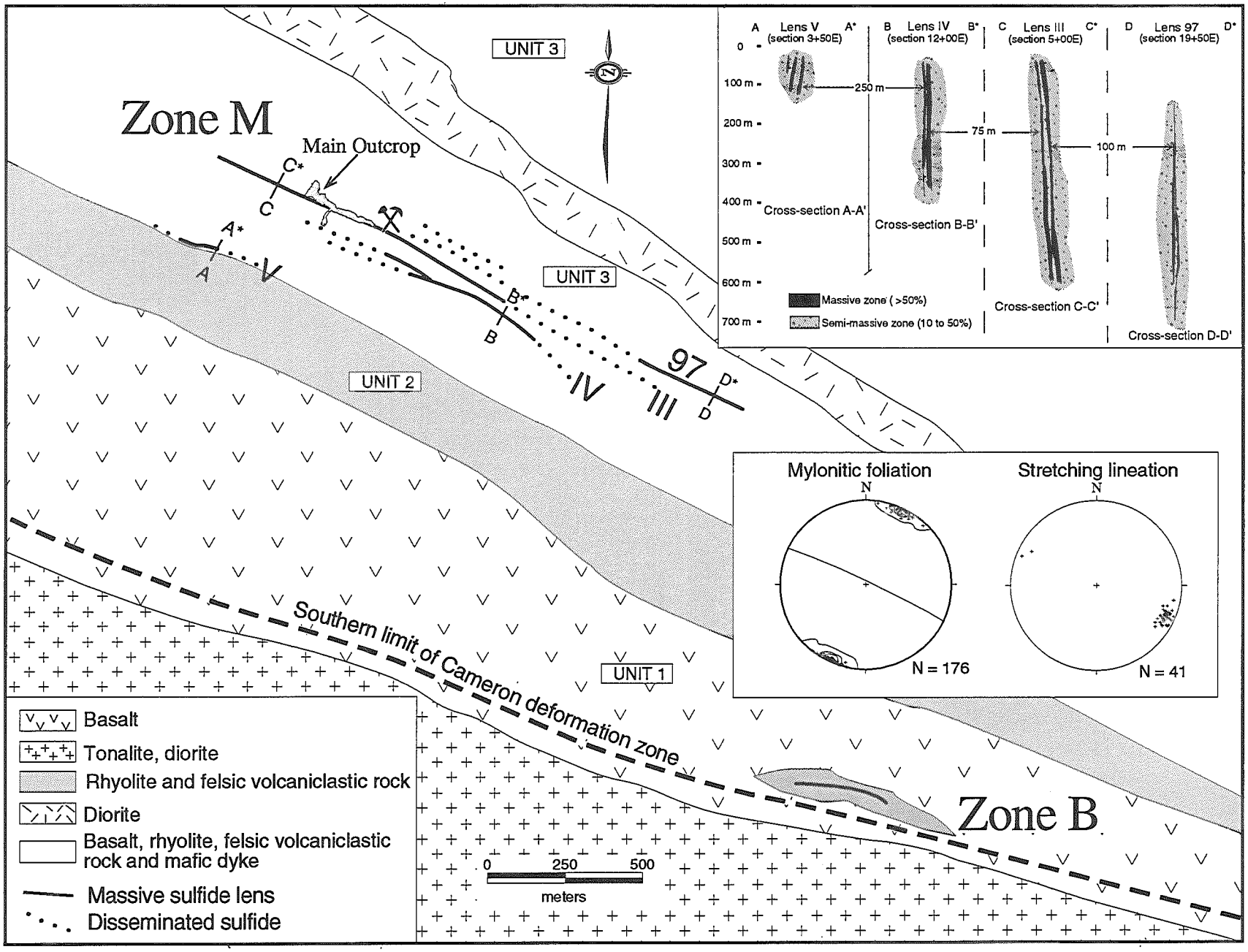

Figure 1. Map of the Grevet deposit with location of the main sulfide lenses. Note the southern boundary of the Cameron deformation zone. The inset shows vertical cross-sections (facing west) throught the main lenses of zone M.

Mine Geology

Lithological units

Due to the limited lateral extent of the various lithologies, and to the high strain intensity, reconstruction of the stratigraphic sequence hosting the ore deposit is difficult. The rock types may be grouped into three lithological units (Fig. 1), which are briefly described from south to north proceeding from the Mountain pluton. The first unit (500 m) consist of a sequence dominated by mafic volcanic rocks showing massive, pillowed and brecciated pillow facies identifiable only where the rocks are least deformed. Unit 2 (250 m) is a sequence consisting of several types of felsic rocks. The felsic package is made up of 3- to 15-m thick alternating bands of massive rock and brecciated facies. Locally, mm-scale quartz phenocrysts are present. Unit 3 (500 m) represents a sequence of alternating horizons of mafic to felsic lava and volcaniclastic rock, transected by several generations of mafic to felsic dykes. The Grevet mine is included in this unit of mixed mafic and felsic rock.

Dykes

Four compositional famillies of dykes are recognized. 1) Plagioclase-phyric gabbroic dykes (3 to 10 m thick), form the most common familly and are characterized by a highly-developed fracture system. These dykes are commonly stretched and dismembered. 2) Fine-grained mafic dykes (1 m thick) are the second familly and exhibit a consistent Z-asymmetry. 3) Diorite dykes (cm- to dm-thick) are the third family and are characterized by intergranular carbonatization. 4) The fourth familly consist of relatively undeformed quartz-feldspar porphyry dykes (10 m thick).

Structural geology

The structure of the Grevet deposit is related intimately to the development of the CDZ, and is typified by intense deformation that all but obliterates primary features of the volcanic and intrusive rocks. The mylonitic foliation, the most penetrative structural element, strikes on average N118° and

dips subvertically (Fig. 2, stereoplot 1). Stretching lineations contained within the mylonitic foliation planes, have a subhorizontal plunge and contrasts markedly with the down-dip stretching lineation outside the CDZ (Lacroix et al. 1993). Shear-sense indicators such as asymmetric pressure shadows and shear bands indicate a dextral component of movement.

Folding and transposition

The structural style of the Grevet deposit is characterized by intense isoclinal folding. The folding results in the near total transposition of volcanic strata, dykes, quartz veins and sulfide lenses, folded layering in volcanic strata, folded sulfide layering, and folded, randomly-oriented fractures and veins within competent dykes. Fold axes are subparallel to the stretching lineation (stereoplot 6 in Fig. 2). The repetitive nature in the mafic and felsic volcanic sequence is interpreted to be the result of transposition. Dm-scale isoclinal folds affecting the primary bedding is observable and axial trace of these folds can be followed consistently for several tens of meters. Asymmetric, Z folds of less than 1 m half-wavelength are systematically associated with dykes of the third familly and are in consequence interpreted to represent transposition of dykes originally oblique to the schistosity.

Folding and transposition of strata combine to produce a tectonic banding parallel to mylonitic foliation. Transposition and accompanying Z-shaped asymmetric folding of strata could have developed in response to dextral shearing characteristic of the CDZ. Parallelism of fold axes and stretching lineations is typical of intense deformation.

A late crenulation cleavage (S_2) striking E-W and dipping subvertically is superimposed on the mylonitic foliation (S_1) over much of the study area. The cleavage, best developed in sericite and chlorite-rich laminae in carbonatized basalt, is associated with the local development of open, cm-scale asymmetric Z-shaped secondary folds. These late folds affect the mylonitic fabric S_1 with subvertical axes (stereoplot 6 in Fig.3), which are perfectly orthogonal to the stretching lineations.

Two late structural features, kink bands and minor faults, transect all other structures. Late stage minor faulting is expressed by the occurrence of metre-scale subvertical dextral shear fractures; oriented on average at N145°, and subordinate, subvertical sinistral shear fractures oriented on

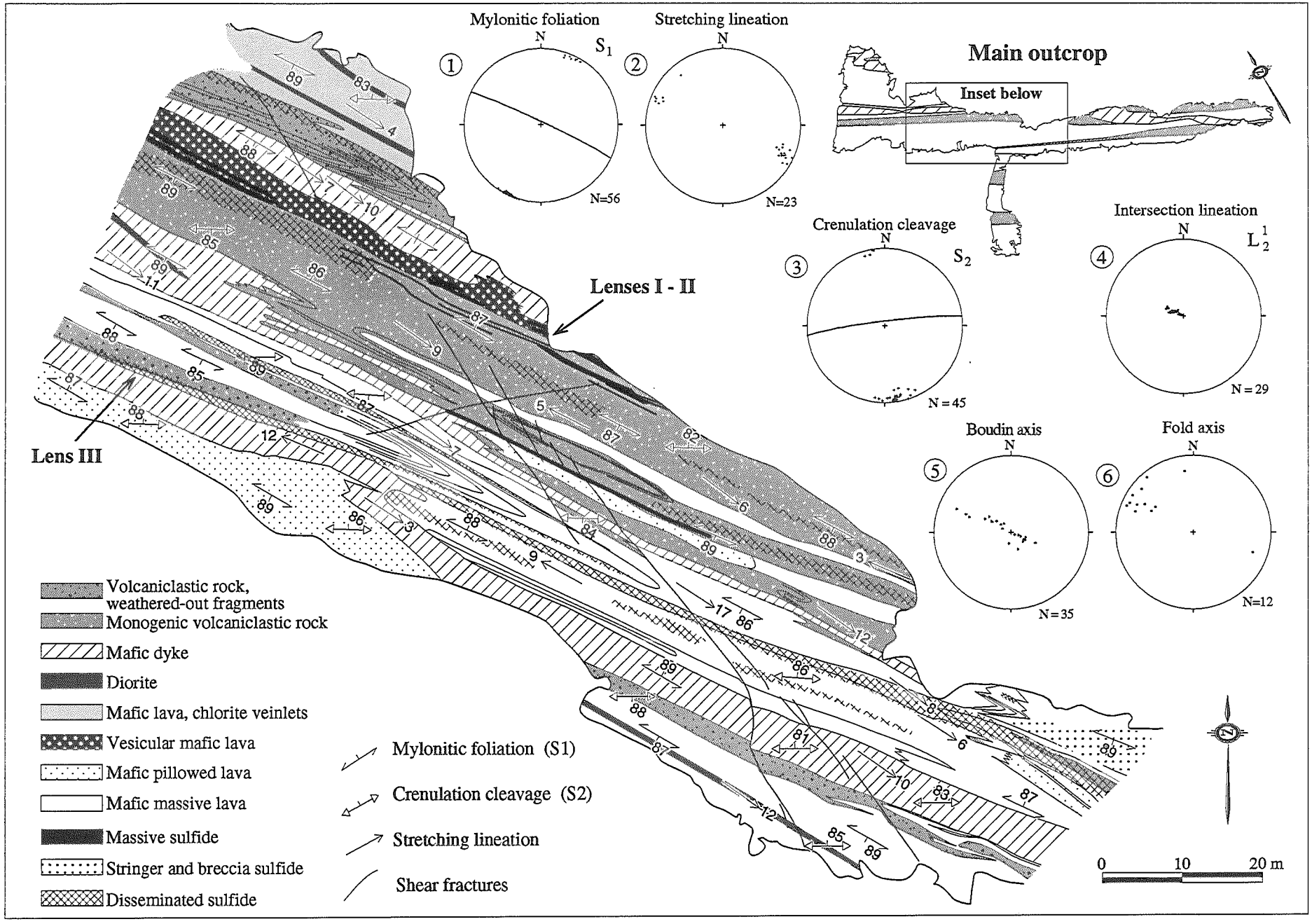

Figure 2. Detailled structural map of the main outcrop near lenses I, II and III. The stereoplots show the attitude of the principal structural elements.

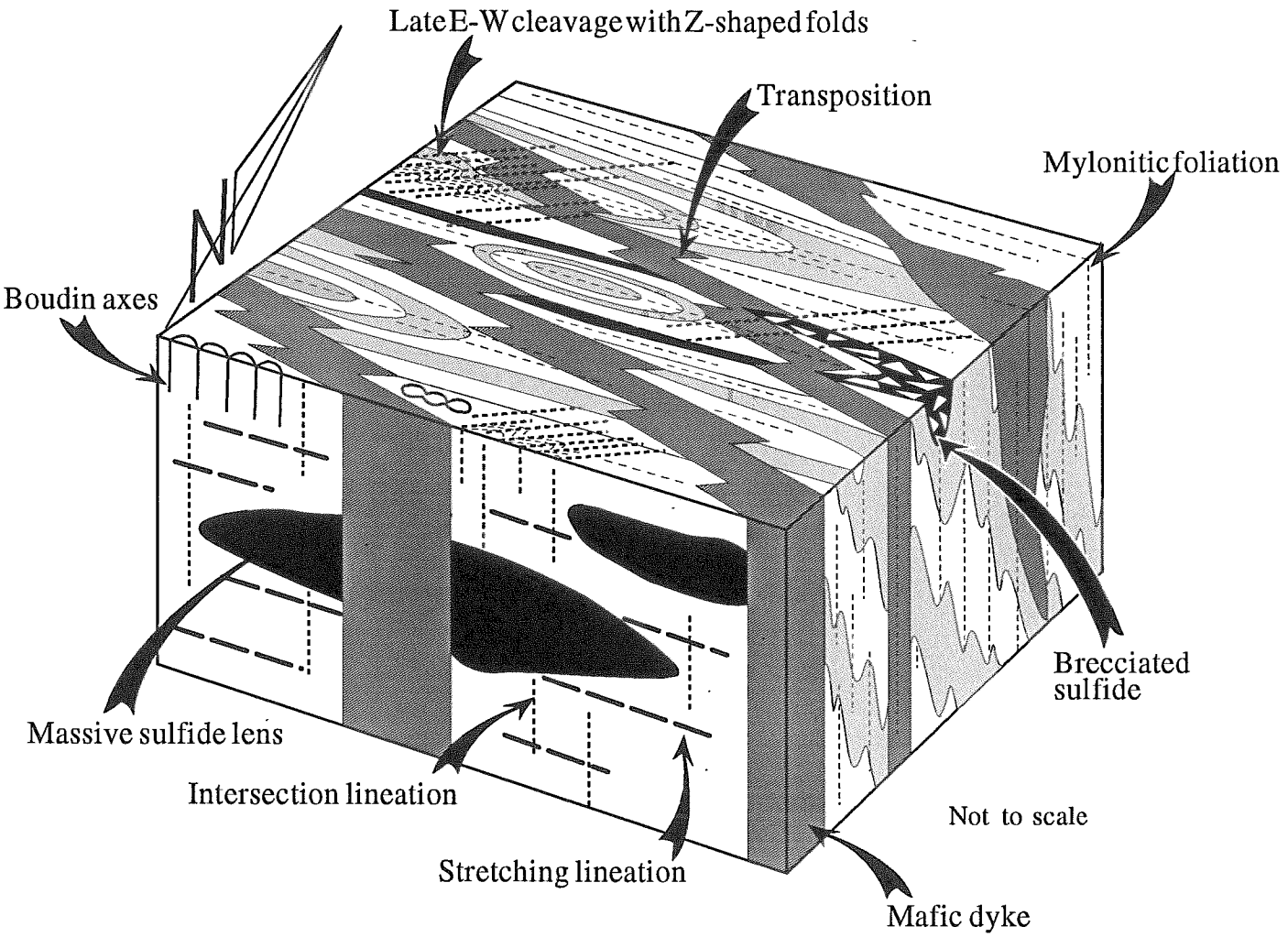

Figure 3. Block diagram summarizing the main structural features for the Grevet deposit.

average at N085°. Kink bands also occur in vertically-dipping conjugate sets which cross-cut the two sets of shear fractures defined above. The dominant set, oriented on average at N228°, is dextral while the subordinate sinistral set strikes on average N184°.

Ore Geology

Base metal mineralization at Grevet occurs as several oblate lenses (Table 1) oriented parallel to the mylonitic foliation. Occurring at approximately 50-100 m intervals across the lithological sequence (Fig. 1), individual sulfide lenses measure several hundred meters along their major axes. Thickness varies from 5 cm to 12 m (Fig. 2). The sulfide lenses consist mainly of sphalerite and pyrite in variable proportions. Primary sulfide textures have been overprinted by recrystallization and deformation textures related to the Cameron deformation zone and regional metamorphism.

Sulfide assemblages

Three different sulfide assemblages are distinguished within the deposit: (1) massive sphalerite and pyrite; (2) stringer and breccia sphalerite and pyrite; and (3) disseminated pyrite (Table 2).

Assemblage 1 is made up by massive sulfide (>90% by volume), comprising variable proportions of sphalerite and pyrite with subordinate pyrrhotite, magnetite, galena, chalcopyrite and arsenopyrite, generally forms lenses several tens of m long and 1 to 7 m thick. Wallrock contacts are generally sharp. Lenses are characterized by sphalerite-pyrite compositional banding and comprises abundant foliated volcanic host rocks enclaves.

Assemblage 2 consists of anastomosing stringers and breccia with rock fragments in a sphalerite and pyrite matrix occur in thin (<2m thick), laterally discontinuous zones (<80% sulfide), that exhibits gradational contacts with the wallrock. Microscopic textural features and megascopic field relations, suggest that the stringer and breccia sulfide assemblage may be formed in part by tectonic brecciation of the massive sulfide assemblage. It is also possible that they represent transposed synvolcanic stockwork zones.

Assemblage 3 consists of disseminated sulfide (<10%) mostly pyrite with minor sphalerite. This

Table 1. Tonnage and grades for reserves of the III, IV, 97 and II lenses of the Grevet M and B zones*

Lens	Metric tonnage (10^6)	Zn (%)	Cu (%)	Lenght (m)	Depth (m)	Average thickness (m)
3	11.27	6.51	0.31	1100	550	4.50
4	3.33	6.46	0.29	600	390	3.61
97	3.38	10.00	0.86	700	1000	3.04
II	0.50	9.37	0.59	300	200	-----

* values valid in 1993

Table 2 - Grevet Sulfide Assemblage (1)

Mineral *	%	Grain size (mm)	Form	Remarks
Pyrite	30 to 70	0.05 to 0.8	Anhedral	-Inclusion in magnetite; 120° triple points; irregular microfractures
		0.5 to 1.3	Anhedral to euhedral	-Contains inclusions of all sulfide minerals
		1.5 to 8	Porphyroblastic	-Brittle behavior; fractured when enclosed in a matrix of pyrrhotite
Sphalerit	30 to 70	?	-Irregular shape -Anhedral to subhedral	-Irregular intergrowth of the pyrite (replacement and inclusion) -Replaces galena
Chalcopyrite	1 to10	0.05 to 0.9	-Oriented blebs and rods - Anhedral	-Interstitial to sphalerite and pyrite
Pyrrhotite	5 to 15	0.03 to ?	Anhedral to subhedral	-Inclusions in pyrite and magnetite; interstitial to included in the sphalerite; deformation twins; in fractures of pyrite
Magnetite	1 to 15	0.02 to 0.7	Anhedral to subhedral	-Interstitial to included in pyrite;disseminated; replacement and inclusion in pyrite
Galena	1 to 2	0.01 to 0.7	Anhedral	-Interstitial to pyrite and sphalerite; inclusions in pyrite and sphalerite
Arsenopyrite	trace	0.02 to 0.2	Anhedral to subhedral	-Inclusions in disseminated pyrite

Sulfide Assemblage (2)

Mineral*	%	Grain size (mm)	Form	Remarks
Pyrite	40 to 70	0.05 to 0.8	Anhedral	-Inclusion in the magnetite -Microfractures irregulieres
		0.5 to 1.3	Anhedral to euhedral	-Contains inclusion of all sulfide minerals
Sphalerite (honey)	10 to 25	0.1 to 4	Anhedral to subhedral Elongate lamellae	-Plastic behavior
Sphalerite (black)	5 to 15	0.05 to 3		
Chalcopyrite	5 to15	0.05 to 4	Anhedral	-Disseminated
Pyrrhotite	5 to 10	0.03 to ?	Anhedral to subhedral	-In fractures of pyrite -Interstitial to included in the sphalerite
Magnetite	5 to 8	0.02 to 0.7	Anhedral to subhedral	-Disseminated -Replacement and inclusion in pyrite

Sulfide Assemblage (3)

Mineral*	%	Size	Form	Remarks
Pyrite	60 to 85	0.05 to 0.8	Anhedral	Disseminated
		0.5 to 1.3	Anhedral to euhedral	Disseminated
Sphalerite	5 to 10	0.1 to 4	Anhedral to subhedral	Disseminated
Magnetite	1 to 5	0.02 to 0.7 mm	Anhedral to subhedral	Disseminated

*listed by decreasing content

sulfide assemblage forms zones several dm-thick and several tens of meters long within and peripheral to the massive and stringer breccia sulfide assemblages. Disseminated sulfides form millimetre-scale laminae parallel to the mylonitic foliation in highly deformed and intensely silicified and sericitized host rock. Pyrite forms individual grains and elongate aggregates, generally with quartz-filled pressure shadows.

Spatial distribution of sulfide assemblages

The main economic lenses in the mine area, lenses 97, III, IV and V, are represented in vertical cross-sections in Figure 1. The mineralized lenses are flattened parallel to the mylonitic foliation and the high-grade envelope plunges easterly at 15° to 20°. This dominant shallow plunge along the lenses long axes coincide well with the attitude of the stretching lineation.

It is important to emphasize the structural relationship between the massive sulfide lenses and the folding event (Figure 2). The symmetrical arrangement of the lenses with respect to the delineated axial fold trace indicates that the lenses were folded in the same way as the lithological units. This spatial distribution of the ore content may be partly or totally a consequence of a structural modification and local remobilization. In addition to exhibiting textures produced by deformation and recrystallisation, sulfide minerals in the three assemblages show evidence of centimetre- to metre-scale remobilization. The evidence includes: (1) sulfide veins and veinlets transecting the wallrock similar to piercement veins described by Maiden et al. (1986); (2) sulfide transecting quartz ribbons, mylonitic foliation and lithological layering; (3) schistose and folded detached wallrock fragments enclosed by massive sulfide; (4) sulfide aggregates occurring within mylonitic foliation planes and within later crenulation cleavage planes. These observations indicate that several pulses of remobilization occurred corresponding to the development of different planar structures during deformation. The presence of sulfide aggregates in synthetic shear bands occupying the stringer/breccia assemblage 2 also suggests sulfide remobilization.

Discussion

The Grevet deposit is hosted by a sequence of extensive submarine plain basalts interpreted as forming the first volcanic cycle in the northern volcanic zone of the Abitibi belt according to Chown et al. (1992). Rocks on the Grevet area may be interpreted as a felsic volcanic submarine edifice associated with a volcanogenic massive sulfide deposits. The deformational history of the Grevet deposit can be differentiated into a sequence of successive shortening and shearing events within the CDZ evolution. A provisional model in which one or several massive sulfide lens are conformable with the host strata is favored. Deformation, resulting in the alternation of sulfide lenses and host lithologies, can explain the repetitive nature of the host rock package (Figure 3). Transposition and décollement surfaces can explain the fact that sulfide lenses are not always hosted by the same rock. It also conceivable that the brecciated and disseminated sulfide assemblages represent an original stringer zones completely transposed by deformation. In the Grevet deposit, observed micro- and meso-scale textures argue for local sulfide remobilization. This remobilization of a limited extent (cm to m-scale) may be produced by mechanical and chemical processes (Gilligan and Marshall, 1987).. A greater extent of remobilization is not demonstrated in the Grevet deposit but could be possible.

References

Chown, E. H., Daigneault, R., Mueller, W., and Mortensen, J. 1992. Tectonic evolution of the Northern Volcanic Zone, Abitibi Belt, Québec. Canadian Journal of Earth Sciences, **29**: 2211-2225.

Daigneault, R., and Archambault, G., 1990, Les grands couloirs de déformation de la sous-Province de l'Abitibi., *In* The Northwestern Quebec Polymetallic Belt. *Edited by* M. Rive, P. Verpealst, Y.

Gagnon, J.M. Lulin, G. Riverin and A. Simard: The Canadian Institute of Mining and Metallurgy, Special Volume 43, p.35-42.

Gilligan, L.B., and Marshall, B., 1987, Textural evidence for remobilization in metamorphic environments., In Mechanical and Chemical
(Re)mobilisation of Metalliferous Mineralization (edited by Marshall, B. and Gilligan, L.B.): Ore Geology Reviews, v.2, p133-173.

Lacroix, J., Daigneault, R., Chartrand, F., and Guha, J. 1993. Structural evolution of the Grevet massive sulphide deposit, Lebel-sur-Quévillon area, Québec. Economic Geology, **88**: 1559-1577.

Maiden, K.J., Chimimba, L.R., Smalley, T.J. 1986, Cuspate ore-wallrock interfaces, piercement structures and the localization of some sulphide ores in deformed sulphide deposits: ECON. GEOL., v.81: 1464-1472.